MOLECULAR AND CELLULAR BIOLOGY, Oct. 2008, p. 5937–5950 Vol. 28, No. 19
0270-7306/08/$08.00+0 doi:10.1128/MCB.00579-08

The AIB1 Oncogene Promotes Breast Cancer Metastasis by Activation of PEA3-Mediated Matrix Metalloproteinase 2 (MMP2) and MMP9 Expression▽

Li Qin,[1]† Lan Liao,[1]† Aisling Redmond,[2] Leonie Young,[2] Yuhui Yuan,[1] Hongwu Chen,[3] Bert W. O'Malley,[1] and Jianming Xu[1]*

Department of Molecular and Cellular Biology and Dan L. Duncan Cancer Center, Baylor College of Medicine, Houston, Texas 77030[1]; Endocrine Oncology Research Group, Department of Surgery, Royal College of Surgeons in Ireland, Dublin, Ireland[2]; and UC Davis Cancer Center/Basic Science, University of California at Davis, Sacramento, California 95817[3]

Received 9 April 2008/Returned for modification 22 May 2008/Accepted 10 July 2008

Amplified-in-breast cancer 1 (AIB1) is an overexpressed transcriptional coactivator in breast cancer. Although overproduced AIB1 is oncogenic, its role and underlying mechanisms in metastasis remain unclear. Here, mammary tumorigenesis and lung metastasis were investigated in wild-type (WT) and AIB1$^{-/-}$ mice harboring the mouse mammary tumor virus-polyomavirus middle T (PyMT) transgene. All WT/PyMT mice developed massive lung metastasis, but AIB1$^{-/-}$/PyMT mice with comparable mammary tumors had significantly less lung metastasis. The recipient mice with transplanted AIB1$^{-/-}$/PyMT tumors also had much less lung metastasis than the recipient mice with transplanted WT/PyMT tumors. WT/PyMT tumor cells expressed mesenchymal markers such as vimentin and N-cadherin, migrated and invaded rapidly, and formed disorganized cellular masses in three-dimensional cultures. In contrast, AIB1$^{-/-}$/PyMT tumor cells maintained epithelial markers such as E-cadherin and ZO-1, migrated and invaded slowly, and still formed polarized acinar structures in three-dimensional cultures. Molecular analyses revealed that AIB1 served as a PEA3 coactivator and formed complexes with PEA3 on matrix metalloproteinase 2 (MMP2) and MMP9 promoters to enhance their expression in both mouse and human breast cancer cells. In 560 human breast tumors, AIB1 expression was found to be positively associated with PEA3, MMP2, and MMP9. These findings suggest a new alternative strategy for controlling the deleterious roles of these MMPs in breast cancer by inhibiting their upstream coregulator AIB1.

The amplified-in-breast cancer 1 (AIB1) (also known as SRC-3, ACTR, and NCOA3) oncogene was initially identified in an amplified chromosomal 20q region in breast cancer cells (19) and subsequently characterized as a member of the p160 steroid receptor coactivator (SRC) family, which also contains SRC-1 and SRC-2 (TIF2 or GRIP1) (1, 8, 36, 46, 54). AIB1 interacts with nuclear hormone receptors such as estrogen and progesterone receptors and certain other transcription factors such as PEA3, E2F1, and AP-1 and serves as a transcriptional coactivator (18, 30, 32, 54). In normal cells, AIB1 usually exists at limiting concentrations. Its coactivator activity is also modulated by posttranslational modifications including phosphorylation, ubiquitination, methylation, and isomerization (14, 52, 57). These modifications are regulated by steroid hormones, growth factors, and cytokines and are associated with cell cycle progression (30, 52, 53, 59). The overexpression or overactivation of AIB1 in breast cancer cells enhances estrogen-induced cyclin D1 expression, epidermal growth factor receptor activation, cell proliferation, and antiestrogen resistance (27, 28, 38, 59). The overexpression of AIB1 in prostate cancer cells increases Akt activation, cell size, and proliferation (61, 62). In addition, AIB1 deficiency dampens insulin-like growth factor I (IGF-I)-stimulated cell proliferation in mouse embryonic fibroblasts and mammary tumor cells (24, 25, 49). Therefore, AIB1 plays an important role in cell growth and survival, and its overexpression and/or activation is a risk factor for tumorigenesis.

The AIB1 gene is amplified in 5 to 10% of human breast cancers, and its mRNA and protein are overexpressed in ~30% of human breast tumors (1, 3, 29). AIB1 overexpression is associated with HER2 expression and poor prognosis in patients treated with tamoxifen (17, 37). Studies using genetic mouse models have further confirmed the crucial role of AIB1 in breast cancer. First, the loss of AIB1 in mice prevents the overactivation of the IGF-I signaling pathway and suppresses mouse mammary tumor virus (MMTV)–v-Ha-ras-induced mammary tumor initiation and progression (25); second, an AIB1 deficiency also makes mammary epithelial cells much more resistant to chemical carcinogens (24); and third, the overexpression of an active AIB1 isoform stimulates mammary epithelial proliferation, and the overexpression of AIB1 causes a high incidence of spontaneous mammary adenocarcinomas (45, 47). These important findings prove that AIB1 is a proto-oncoprotein.

AIB1 is involved in cell migration. For example, the loss of Taiman, a *Drosophila* protein related to AIB1, arrested the border cell migration in the *Drosophila* ovary (2); also, AIB1 deficiency reduced levels of mammary tumor cell migration (25). However, the exact contribution and molecular mecha-

* Corresponding author. Mailing address: Department of Molecular and Cellular Biology, Baylor College of Medicine, 1 Baylor Plaza, Houston, TX 77030. Phone: (713) 798-6199. Fax: (713) 798-3017. E-mail: jxu@bcm.tmc.edu.

† L.Q. and L.L. contributed equally to this work.

▽ Published ahead of print on 21 July 2008.

nisms for AIB1 in the regulation of breast cancer metastasis are unknown. In this study, we have used the MMTV-polyomavirus middle T antigen (PyMT) transgenic mouse model for lung metastasis (20) to characterize the role of AIB1 in mammary tumor progression and metastasis. We report that the AIB1 deficiency significantly reduces mammary tumor metastasis in the lung. AIB1-deficient tumor cells have a more differentiated phenotype in three-dimensional (3D) culture, and the loss of AIB1 inhibits the epithelial-mesenchymal transition (EMT) and reduces tumor cell migration and invasion during tumor progression. These observations are associated with suppressed expression and activities of matrix metalloproteinase 2 (MMP2) and MMP9. We also demonstrate that AIB1, as a PEA3 coactivator, directly promotes MMP2 and MMP9 expression and that the expression levels of AIB1, PEA3, MMP2, and MMP9 are associated in human breast cancers.

MATERIALS AND METHODS

Mammary tumorigenesis in bitransgenic mice. Animal protocols were approved by the Animal Care and Use Committee of Baylor College of Medicine. AIB1 mutant mice with a backcrossed FVB background were described previously (24). MMTV-PyMT mice with an FVB background (20) were obtained from the Jackson Laboratory. Their genotypes were analyzed by PCR as described previously (20, 55). AIB1$^{+/-}$ females and PyMT males were crossbred for two generations to produce wild-type (WT)/PyMT and AIB1$^{-/-}$/PyMT mice. Female mice were examined weekly to detect palpable mammary tumors. The tumor length (L) and width (W) were measured weekly, its volume was calculated by the equation $(L \times W^2)/2$, and tumor-free curve and log-rank tests were done as described previously (60). Mice were sacrificed 8 weeks after palpable tumors were detected. Tumors and lungs were isolated and fixed for histological examination as described previously (25, 60).

Mammary tumor transplantation. Mammary tumors of similar sizes were isolated from WT/PyMT and AIB1$^{-/-}$/PyMT donor mice and cut into small pieces (~2 mm in diameter). Female WT recipients (3 to 4 months old) were anesthetized with avertin, and both inguinal mammary glands of these mice were implanted with a piece of WT/PyMT or AIB1$^{-/-}$/PyMT tumor tissue as described previously (60). Tumor growth was measured weekly, and recipient mice were sacrificed 8 weeks after transplantation. Tumors and lungs were isolated from these recipient mice for histological examination.

Examination of lung metastasis. Mouse lungs were isolated and examined under a stereomicroscope for visible focal tumors. Lung sections were stained with hematoxylin and eosin (H&E). Lung metastasis was determined by examining focal tumors on three sagittal lung sections spaced 300 μm between sections. Tumor and normal lung tissue areas were measured using software as described previously (25).

IHC. Tumor tissues were fixed in 4% paraformaldehyde. Tissue sections were cut at a thickness of 6 μm, deparaffinized, and stained with H&E. For immunohistochemistry (IHC), rehydrated sections were incubated overnight at 4°C with primary antibodies against E-cadherin, β-catenin, N-cadherin (BD Biosciences), MMP2 (Chemicon), or MMP9 (Santa Cruz Biotechnology). The immunostaining signal was made visible using the ABC kit containing the diaminobenzidine substrate for horseradish peroxidase (Vector Laboratories).

Development of mammary tumor cell lines. Individual mammary tumors were isolated from WT/PyMT and AIB1$^{-/-}$/PyMT mice and minced in Dulbecco's modified Eagle's medium (DMEM) with 1 mg/ml collagenase A. The minced tissues were digested overnight at 37°C in the same solution and pipetted up and down into cell suspension. The cells were cultured overnight in DMEM with 10% fetal calf serum (FCS), 10 μg/ml insulin, and 0.1 mM β-mercaptoethanol for initial attachment and then cultured in serum-free medium from an MEGM Bullet kit (Lonza Inc.) for 20 passages. The epithelial marker cytokeratin 8 (CK8) was detected in 95 to 100% cells of these established lines by IHC.

3D culture. The 3D culture of WT/PyMT and AIB1$^{-/-}$/PyMT cells was performed as described previously (11). Five thousand cells in 400 μl of DMEM containing 2% FCS, 5 ng/ml epidermal growth factor (EGF), and 2% Matrigel were seeded onto the Growth Factor Reduced Matrigel matrix in eight-well chamber slides (BD Biosciences) and cultured for 8 to 18 days. The medium was changed every 4 days. Cells were fixed in methanol and acetone (1:1) and blocked in phosphate-buffered saline containing 0.1% bovine serum albumin, 0.2% Triton X-100, 0.05% Tween 20, and 10% goat serum for 1.5 h. For immunofluorescence staining, cells were first incubated overnight with antibodies against E-cadherin, N-cadherin (BD Biosciences), or ZO-1 (Zymed Laboratories) at 4°C and then incubated with fluorescent conjugated secondary antibodies at room temperature for 45 min. After counterstaining with TO-PRO-3 or propidium iodide, the slides were mounted in 50% glycerol and examined by confocal microscopy.

Cell motility and invasion assays. For motility assay, the phagokinetic tracks cleared by individual cells in a fibronectin-coated 96-well plate were traced for 18 h using blue fluorescent beads as described previously (59). Cells were fixed in 5.5% formaldehyde, stained with rhodamine-phalloidin, and examined under a fluorescence microscope. Five electronic images were taken for each sample, and track areas were quantitatively analyzed by NIH image software as described previously (59). A cell invasion assay was performed with BioCoat Matrigel invasion chambers (BD Biosciences) as described previously (59). Cells (25,000 cells/well) were loaded into the upper chambers with serum-free medium, and the lower chambers were filled with culture medium with 5% FCS. Cells were cultured for 22 h. Cells that had invaded through the Matrigel layer and crossed the membrane with 8-μm pores were fixed, stained, and counted.

Gelatin zymography assay. MMP2 and MMP9 activities were assayed as described previously (16). Briefly, 0.5×10^6 cells in a 12-well plate were cultured for 24 h in DMEM with 0.1% FCS, and the conditioned medium was collected. Cells were lysed in radioimmunoprecipitation assay buffer, and total cellular protein was measured. The amount of medium conditioned by the same number of cells (~40 μg of cellular protein) was mixed with loading buffer containing 8% sodium dodecyl sulfate (SDS)–40% glycerol–0.04% bromophenol blue and 0.25 M Tris-HCl (pH 6.8) and separated in a 10% SDS-polyacrylamide gel electrophoresis (PAGE) gel containing 1 mg/ml gelatin. The gel was washed with buffer I (Tris-HCl [pH 7.5] and 2.5% Triton X-100) and incubated overnight in buffer II (150 mM NaCl, 5 mM $CaCl_2$, 50 mM Tris-HCl [pH 7.6]) at 37°C. The gel was stained with Coomassie blue. The brightness of clear bands, where MMPs were located and gelatin was degraded, was analyzed by densitometry.

Real-time reverse transcription-PCR (qPCR). Total RNA was isolated from cells using TRIzol reagents (Invitrogen). Reverse transcription was performed with 1 μg RNA using a reverse transcriptase core kit (Eurogentec). Mouse MMP2 (mMMP2), mMMP9, mAIB1, mPEA3, human MMP2 (hMMP2), hMMP9, and hAIB1 mRNAs were measured by quantitative PCR (qPCR) using specific TaqMan probes and gene-specific primers (Table 1). The measurement of β-actin mRNA was used as an endogenous control.

AIB1 knockdown and adenovirus-mediated expression. For AIB1 knockdown, WT/PyMT and MDA-MB-231 cells (5×10^5 cells in a six-well plate) were transfected with the small interfering RNA (siRNA) smart pool for human or mouse AIB1 or scrambled control siRNA (Dharmacon) using Transit-TKO transfection reagent (Mirus). Knockdown efficiency was examined by qPCR and Western blotting. For AIB1 expression, AIB1$^{-/-}$/PyMT cells were infected with adenoviruses carrying either an AIB1 or a green fluorescent protein (GFP) control expression cassette as described previously (30). Adenovirus-mediated AIB1 expression was examined by Western blotting. Cells were lysed in radioimmunoprecipitation assay buffer at 4°C. The cell lysates were used for Western blotting as described previously (9).

Cell transfection and luciferase assays. The pGL2-MMP2-Luc promoter/reporter construct was described previously (6). The pGL3-MMP9-Luc promoter/reporter plasmid was constructed with a 1,305-bp DNA fragment amplified by PCR from the proximal promoter/enhancer region of the human MMP9 gene based on a previous report (21). The PCR primers were 5′-TGGTACCGGGA GGGAGGCTTGGCATAAG and 5′-TAAGCTTGGTGGGGCAGAGGTGT CTG. WT/PyMT and AIB1$^{-/-}$/PyMT cells in a 12-well plate with 80% confluence were transiently transfected with plasmids pGL2-MMP2-Luc or PGL3-MMP9-Luc and pSV40-gal using Lipofectamine 2000 Plus reagent (Invitrogen). pSV40-gal constitutively expressed β-galactosidase (β-gal), which was used to normalize transfection efficiency. HeLa cells were cotransfected with pSV40-gal, pCR3.1-AIB1, and pGL2-MMP2-Luc (or pGL3-MMP9-Luc) and the expression plasmids of PEA3, NF-κB, or c-Jun. Total DNA for each well was added to the same amount using their respective parent vectors when different combinations of plasmids were applied. Cells were cultured for 48 h and then lysed in reporter assay lysis buffer (Promega). Luciferase activity was assayed using a luciferase assay system (Promega). β-gal activity was assayed as described previously (35). Relative luciferase activity was normalized to β-gal activity.

Co-IP. Cell lysates prepared from WT/PyMT, AIB1$^{-/-}$/PyMT, and MDA-MB-231 cells were subjected to coimmunoprecipitation (co-IP) using 2 μg of AIB1 or PEA3 antibody. An equal amount of immunoglobulin G (IgG) was used as a negative control. Immunocomplexes were denatured and separated in SDS-

TABLE 1. Sequences of synthetic oligonucleotides

Primer name	Primer sequence	
	Forward	Reverse
For ChIP assays		
hMMP2-a	5′-TCAGAGACGGTTGTCACAGG	5′-GTTAAAGGAAGCACCCACCA
hMMP2-b	5′-CCCCTGTTCAAGATGGAGTC	5′-CCCAGGTTGCTTCCTTACCT
hMMP2-c	5′-ACCGCTGCTCTCTAACCTCA	5′-CCCTCCTCCACTTTTCTCCT
hMMP9-a	5′-CTTCAGAGCCAGGCAGTTCT	5′-AGCCTCTCGTTTCATCCTCA
hMMP9-b	5′-TAATTGGGCCTGGAGATTTG	5′-CCTGCCAAAAGACCATGATT
hMMP9-c	5′-TAAGACATTTGCCCGAGGTC	5′-CCTCTTTTTCCCTCCCTGAC
hMMP9-d	5′-GGAGGTGGTGTAAGCCCTTT	5′-AGGGCAGAGGTGTCTGACTG
mMMP2-a	5′-CCTGAAGTTCATCTTCCCCTGATTC	5′-ATGAACCTTCTCTTCCTCCACAAGG
mMMP2-b	5′-ATTCCCCTTTCTCACTCACAGGAAC	5′-CGTCCCTGGTAAGTGTTCTTTCCTT
mMMP2-c	5′-GTTTGGAGAAGGAAGGCTGGTTAGA	5′-TTTGGAGGGATACTGGAATCAGGAC
mMMP9-a	5′-CAGGAGGCTTAGTCAGAACAGCTTG	5′-GAGACCTCAGTTGATGGTGTCAGGT
mMMP9-b	5′-AGTGCTAGCCTGAGAAGGATGAAGC	5′-CCCATCCCCACACTGTAGGTTCTAT
Real-time reverse transcription-PCR		
mPEA3	5′-TTGTTCCTGATTTCCATTCAGA	5′-GACTCTGGGGTTCCTTCTTGA
hMMP2	5′-CCGTCGCCCATCATCAA	5′-AGATATTGCACTGCCAACTCT
hMMP9	5′-TCGTGGTTCCAACTCGGTTT	5′-GCGGCCCTCGAAGATGA
mMMP2	5′-TCTGCGATGAGCTTAGGGAAAC	5′-GACATACATCTTTGCAGGAGACAAG
mMMP9	5′-GGACGACGTGGGCTACGT	5′-CACGGTTGAAGCAAAGAAGGA
hAIB1	5′-CAGTCCTGAAATGCGCCAG	5′-CGGCGTGCCACACAGAT
mAIB1	5′-AGCAAAGGCCACAAGAAACTG	5′-GGTCAAGGAGGAATGGCCTC

PAGE gels for Western blotting using AIB1 and PEA3 antibodies. All co-IP assays were repeated three times.

ChIP and ChIP-re-ChIP. WT/PyMT, AIB1$^{-/-}$/PyMT, and MDA-MB-231 cells (2×10^7 cells) were cross-linked in 1% formaldehyde, lysed in 0.6 ml of lysis buffer, and sonicated as described previously (44). Cell lysates were precleaned with protein G/A beads, and 20 μl of each lysate was saved as an input control. The remaining lysates were subjected to immunoprecipitation using 2 μg of AIB1 or PEA3 antibody and protein G/A beads. For the chromatin immunoprecipitation (ChIP)-re-ChIP assay, the PEA3-DNA complexes immunoprecipitated by PEA3 antibody were eluted in 1% SDS, diluted 10 times in immunoprecipitation buffer, and reimmunoprecipitated with AIB1 antibody. Immunoprecipitates were eluted, digested with proteinase K, and incubated at 65°C. DNA was extracted using phenol-chloroform as described previously (44). PCR was performed to amplify mouse and human MMP2 and MMP9 promoter fragments using specific primer pairs (Table 1). All ChIP assays were repeated three or more times.

IHC for AIB1, PEA3, MMP2, and MMP9 in human breast tumors. A total of 560 breast tumor samples from archival cases from 1987 to 1999 at St. Vincent's University Hospital were collected from primary surgeries before endocrine therapy. After surgery, patients received either no endocrine treatment ($n = 200$) or 20 mg/day of tamoxifen ($n = 360$) for 5 years, which was discontinued only for those patients who suffered a relapse while on endocrine therapy. Excluded from the analysis were patients who did not have breast surgery, those who had neoadjuvant therapy, or those whose tissue specimens were irretrievable. Data for the patients included pathological characteristics (tumor size, grade, lymph node status, and estrogen receptor status) as well as treatment with radiotherapy, chemotherapy, or tamoxifen. Archival tissue was attained for the patient population for the purposes of tissue microarray construction. An H&E-stained slide was used for all specimens to mark the site of carcinoma. Three 0.6-mm punch biopsies were taken from each specimen and transplanted into a recipient block. Tissue array sections (5-μm thickness) were prepared from the recipient blocks, mounted onto Superfrost Plus slides (BDH, Poole, United Kingdom), and baked for 1 h at 60°C. For IHC, rehydrated sections were incubated in 3% H_2O_2 for two 10-min immersions in the dark and microwaved in 0.01 M sodium citrate for 7 min. Sections were blocked in FCS for 90 min. All primary antibodies were diluted in phosphate-buffered saline. Sections were incubated for 1 h at room temperature with control IgG or the following primary antibodies: rabbit anti-human AIB1 (3 μg/ml) (Santa Cruz, CA), mouse anti-human MMP2 (5 μg/ml) (Thermo Scientific, Fremont, CA), mouse anti-human MMP9 (2 μg/ml) (Chemicon, Temecula, CA), and mouse anti-human PEA3 (50 μg/ml) (Santa Cruz, CA). Sections were subsequently incubated with the appropriate biotin-labeled secondary antibodies for 30 min, followed by a peroxidase-labeled avidin-biotin complex (Vector Laboratories, Burlingame, CA) for 30 min. Sections were developed in 3,3-diaminobenzidine tetrahydrochloride for 8 min and counterstained with hematoxylin for 3 min. The stained sections were dehydrated, treated with xylene, and mounted for examination. Statistical analysis was carried out using the Fisher's exact test for categorical variables to compare two proportions. Kaplan-Meier estimates of survival functions were computed, and the Wilcoxon test was used to compare survival curves. In addition, the Wilcoxon rank sum test was used to compare two medians. Two-sided P values of <0.05 were considered to be statistically significant.

RESULTS

Genetic ablation of AIB1 suppresses lung metastases of mammary tumors. To investigate the role of AIB1 in mammary tumorigenesis and breast cancer metastasis, we crossed AIB1$^{-/-}$ mice with MMTV-PyMT mice and produced female WT/PyMT and AIB1$^{-/-}$/PyMT bigenic mice. qPCR analyses confirmed that AIB1 was expressed in the mammary glands and livers of WT/PyMT mice, but its expression was undetectable in the mammary glands of AIB1$^{-/-}$/PyMT mice (Fig. 1A). PyMT was comparably expressed in the mammary glands and tumors of WT/PyMT and AIB1$^{-/-}$/PyMT mice, suggesting that AIB1 deficiency does not affect MMTV-PyMT transgene expression. As a negative control, PyMT expression was not detectable in the livers of nontransgenic mice (Fig. 1B and data not shown). In WT/PyMT mice, palpable mammary tumors were detected from 35 to 92 days of ages, with a median value of 60 days. However, palpable mammary tumors in AIB1$^{-/-}$/PyMT mice were detected only at older ages, which were from 62 to 137 days of age, with a median value of 92 days (Fig. 1C). Mammary tumor growths showed significant variations in both groups of mice. Although the average growth rate of WT/PyMT mammary tumors was slightly faster than that of AIB1$^{-/-}$/PyMT tumors, their difference was not statistically significant (Fig. 1D). Therefore, AIB1 deficiency mainly extends the latency of PyMT-induced mammary tumorigenesis.

To investigate the role of AIB1 in breast cancer metastasis,

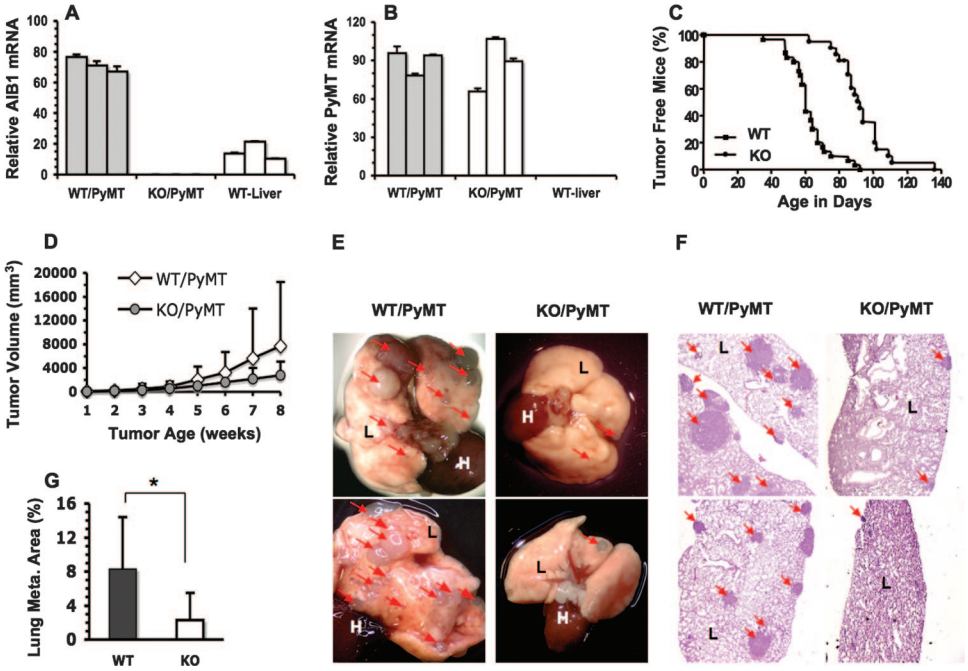

FIG. 1. AIB1 deficiency extends mammary tumorigenic latency and suppresses lung metastasis in MMTV-PyMT mice. (A) Relative AIB1 mRNA levels in the mammary glands of WT/PyMT and KO (AIB1$^{-/-}$)/PyMT mice. The livers of WT mice served as a positive control. Triplicate qPCR measurements were performed for each mouse sample, and three samples were measured. (B) PyMT expression levels in mammary glands of WT/PyMT and KO/PyMT mice. The livers of WT mice served as a negative control. (C) Tumor-free curves for WT/PyMT (WT) ($n = 30$) and KO/PyMT (KO) ($n = 21$) mice. Palpable mammary tumor formation was delayed in KO/PyMT mice ($P < 0.0001$ by log-rank test). (D) Tumor growth in WT/PyMT and KO/PyMT mice. Mammary tumor volumes were measured once a palpable tumor was detected. A total of 28 WT/PyMT and 20 KO/PyMT tumors were monitored. There was no statistical difference in the growth rates of these two types of tumors. (E) Lung images. The lungs of WT/PyMT mice had many more focal tumors (arrow heads) than did the lungs of KO/PyMT mice. L, lung; H, heart. (F) H&E-stained lung sections from different WT/PyMT and KO/PyMT mice. L, lung tissue; arrowheads, metastatic lung tumors. (G) The percentage of lung metastasis area to total lung area in WT/PyMT (WT) mice ($n = 8$) was much higher than that in KO/PyMT (KO) mice ($n = 8$). *, $P < 0.05$ by unpaired t test.

we examined the frequency and extent of lung metastasis in WT/PyMT and AIB1$^{-/-}$/PyMT mice. Mice were sacrificed when they had borne palpable mammary tumors for 8 weeks, so both WT/PyMT and AIB1$^{-/-}$/PyMT mice had mammary tumors with comparable time periods and sizes at the experimental endpoint. Numerous small and large metastatic tumors were observed from the lung surfaces of all WT/PyMT mice examined. In contrast, only several small metastatic tumors were observed on the lung surfaces of 71% (12 out of 17) of AIB1$^{-/-}$/PyMT mice (Fig. 1E). To quantify the extent of lung metastasis, for each lung sample, we prepared three lung sections with 100-μm intervals to each other for measuring metastatic tumor areas and total lung section areas. Metastatic tumors were found in lung sections from eight of eight WT/PyMT mice and seven of eight AIB1$^{-/-}$/PyMT mice. Strikingly, the tumor areas in AIB1$^{-/-}$/PyMT lung sections were much smaller than those in WT/PyMT lung sections (Fig. 1F). The average tumor areas were 8.5% and 2.5% of the total lung section areas in WT/PyMT and AIB1$^{-/-}$/PyMT mice, respectively (Fig. 1G). These results demonstrate that the genetic ablation of AIB1 drastically reduces mammary tumor metastasis in the lung in MMTV-PyMT mice.

AIB1 in mammary tumor cells is required for lung metastasis in normal recipient mice. To test the intrinsic role of AIB1 in metastasis, we transplanted small pieces of WT/PyMT and AIB1$^{-/-}$/PyMT mammary tumor tissues to the mammary fat pads of nontransgenic normal mice and compared local tumor growth and lung metastasis in these recipient mice. The average growth rates of the transplanted WT/PyMT and AIB1$^{-/-}$/PyMT tumors in the mammary fat pads did not show a significant difference (Fig. 2A). However, remarkable differences in lung metastases were observed (Fig. 2B). At 8 weeks after transplantation, several to numerous metastatic tumors were observed on all lung surfaces of recipient mice with WT/PyMT mammary tumors. In contrast, only a few tumors were found on the lung surfaces of 50% (four of eight) of recipient mice with AIB1$^{-/-}$/PyMT mammary tumors (Fig. 2B). The other 50% of recipient mice with AIB1$^{-/-}$/PyMT mammary tumors did not develop any lung metastasis (Fig. 2B to D). Measurements with lung sections revealed that the average metastatic lung tumor area in mice with AIB1$^{-/-}$/PyMT mammary tumors was more than ninefold smaller than that in mice with WT/PyMT mammary tumors (Fig. 2C and D). These results indicate that AIB1 is required for lung metastasis in the tumor cell.

AIB1$^{-/-}$ tumor cells exhibit a more differentiated epithelial phenotype. During breast cancer progression, invasive and metastatic tumor cells usually reduce or stop the expression of certain epithelial markers such as E-cadherin and β-catenin, start to express mesenchymal markers such as N-cadherin and

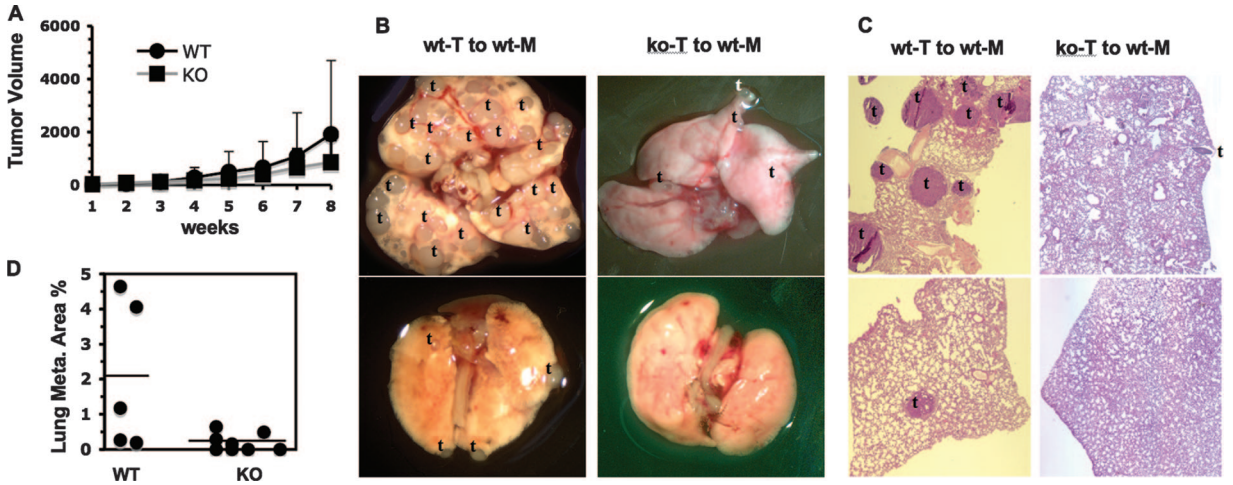

FIG. 2. Transplanted AIB1$^{-/-}$/PyMT tumors result in much less metastasis than transplanted WT/PyMT tumors in normal recipient mice. (A) Growth curves of transplanted WT/PyMT (WT) and AIB1$^{-/-}$/PyMT (KO) tumor tissues in normal female recipient mice. The volumes (mm^3) of 18 WT/PyMT and KO/PyMT tumors were measured and showed no statistical difference between two groups ($P > 0.05$). (B) Representative lung images of recipient mice (wt-M) bearing implanted WT/PyMT (wt-T) or AIB1$^{-/-}$/PyMT (ko-T) mammary tumors. Mice with WT/PyMT mammary tumors had extensive lung metastasis as indicated by the letter t. (C) H&E-stained lung sections from different recipient mice with WT/PyMT or AIB1$^{-/-}$/PyMT mammary tumors. The focal tumors of lung metastasis are indicated by the letter t. (D) Percentage of lung tumor area to total lung area. Lung samples were prepared from five and eight recipient mice with WT/PyMT (WT) and AIB1$^{-/-}$/PyMT (KO) mammary tumors. The horizontal lines mark the average values of each group. The unpaired *t* test showed a significant difference ($P < 0.05$) between the two groups.

vimentin, and lose epithelial polarity (50). Indeed, most WT/PyMT mammary tumor cells expressed low levels of or no E-cadherin and β-catenin and high levels of N-cadherin and vimentin. In contrast, most AIB1$^{-/-}$/PyMT mammary tumor cells maintained E-cadherin and β-catenin expression and expressed little or no N-cadherin and vimentin as assayed by IHC and Western blot assays (Fig. 3A and C). To examine the role of AIB1 in mammary tumor cell behavior, we developed two cell lines from WT/PyMT and two cell lines from AIB1$^{-/-}$/PyMT mammary tumors isolated from different mice. Immunocytochemistry confirmed that all of these cell lines had an epithelial origin because they expressed the epithelial marker CK8 (Fig. 3B). By day 8 in the 3D culture system, single WT/PyMT tumor cells seeded in the growth factor-reduced Matrigel proliferated and sprouted to form an undifferentiated dendritic architecture (Fig. 3D). By day 18 in the 3D culture, both lines of the WT/PyMT tumor cells failed to form differentiated acinar structures. Instead, they formed invasive cellular masses consisting of strands of tumor cells expressing low levels of unpolarized ZO-1 and E-cadherin and high levels of N-cadherin (Fig. 3D). ZO-1 is a tight-junction protein normally located at the apilateral membrane of polarized epithelial cells (23). These cellular and molecular features are consistent with the highly metastatic phenotype of WT/PyMT mammary tumors in mice and are commonly observed in invasive human cancer cells. Surprisingly, under identical 3D culture conditions, individual cells of both lines of AIB1$^{-/-}$/PyMT cells underwent 3D morphogenesis and developed mammary epithelial spheres by day 8. By day 18, these cells formed highly differentiated hollow spheres consisting of a single layer of polarized epithelial cells. In these spheres, ZO-1 was seen on the luminal surface of the epithelial layer; E-cadherin was seen between epithelial cells, which maintained the interaction between these cells; and N-cadherin was undetectable (Fig. 3D). Taken together, these results indicate that AIB1$^{-/-}$/PyMT tumor cells are much more differentiated epithelial cells than are WT/PyMT tumor cells. Thus, we conclude that AIB1 is required for mammary tumor cells to progress to a more malignant stage.

AIB1 deficiency suppresses mammary tumor cell migration and invasion. Cell migration and invasion capabilities usually correlate with cancer metastasis. To examine if AIB1 promotes cell migration, we seeded WT/PyMT and AIB1$^{-/-}$/PyMT cells on fluorescent bead-coated plates and traced the phagokinetic tracks of individual cells in an 18-h period. Most WT/PyMT cells migrated much faster than did AIB1$^{-/-}$/PyMT cells (Fig. 4A). A computer-assisted quantitative measurement revealed that the average areas of phagokinetic tracks made by two independent AIB1$^{-/-}$/PyMT cell lines were drastically reduced ($P < 0.0001$) compared with those made by two independent WT/PyMT cell lines (Fig. 4B). Cell invasion capabilities of WT/PyMT and AIB1$^{-/-}$/PyMT cells were also compared in Matrigel-coated invasion assay chambers using 5% FCS as a chemoattractant. Within 22 h, as many as 55% and 35% cells of the two WT/PyMT lines invaded through the Matrigel layer. In contrast, only 8% and 14% of cells of the two AIB1$^{-/-}$/PyMT lines invaded through the Matrigel layer, which were significantly lower than the migration ratios of WT/PyMT cells (Fig. 4C). These results demonstrate that AIB1 plays an important role in the promotion of mammary tumor cell migration and invasion.

AIB1 deficiency reduces MMP2 and MMP9 expression levels in mammary tumors and cell lines. Growth factor and cytokine pathways and MMPs have been shown to regulate cell migration and invasion. Our previous studies have shown that AIB1 deficiency attenuates IGF-I signaling by reducing the

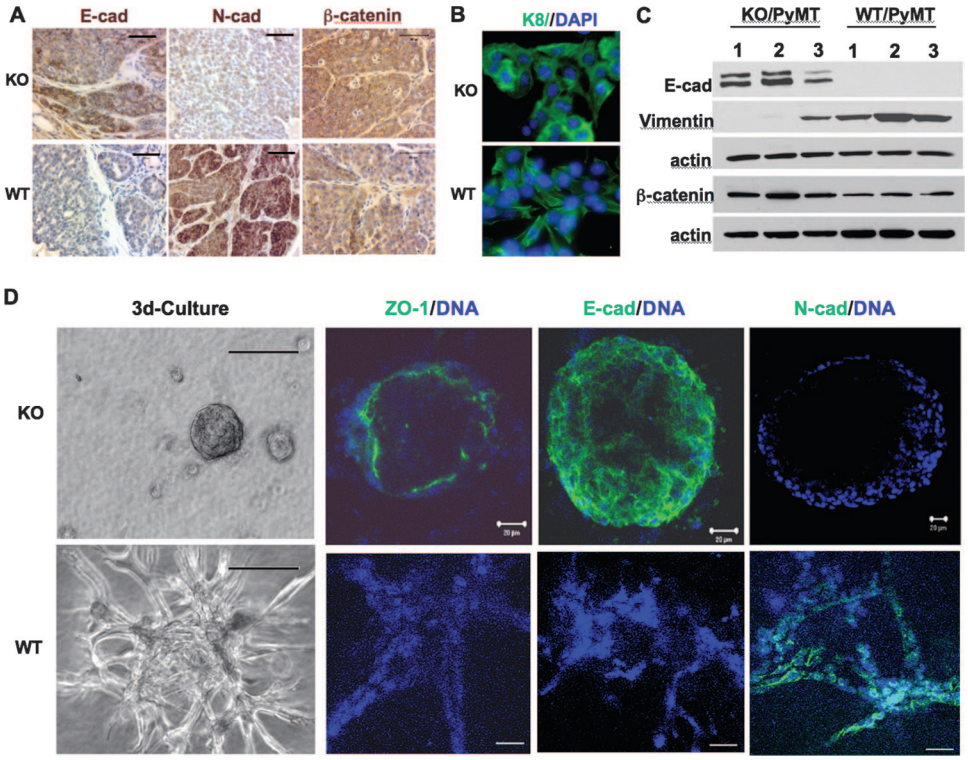

FIG. 3. AIB1$^{-/-}$/PyMT tumor cells are more differentiated and less malignant than WT/PyMT tumor cells. (A) IHC for E-cadherin (E-cad), N-cadherin, and β-catenin (brown) in AIB1$^{-/-}$/PyMT (KO) and WT/PyMT (WT) mammary tumors. Scale bars, 50 μm. (B) Immunofluorescent staining for CK8 (green) in AIB1$^{-/-}$/PyMT and WT/PyMT mammary tumor cell lines. DAPI, 4′,6′-diamidino-2-phenylindole. (C) Western blot analysis of E-cadherin, vimentin, and β-catenin in three AIB1$^{-/-}$ (KO)/PyMT and WT/PyMT tumor cell lines. β-Actin serves as a loading control. (D) Morphologies and characteristic markers of AIB1$^{-/-}$/PyMT and WT/PyMT tumor cells in 3D cultures. Cells were cultured for 18 days and imaged under a phase-contrast microscope (left). Immunofluorescent staining was performed with antibodies against ZO-1, E-cadherin, and N-cadherin. Cell nuclei were visualized by TO-PRO-3 staining. Fluorescence-labeled 3D cultures were examined and imaged under a confocal microscope. Scale bars, 100 μm (left) and 20 μm (other panels).

expression of IGF-I, insulin receptor substance 1 (IRS-1), and IRS-2 and inhibiting Akt activation, which could partially explain why AIB1 deficiency reduced cancer cell migration and metastasis (25, 26). Here, we examined the expression levels of epidermal growth factor receptor, transforming growth factor β receptors (TGFβRI and TGFβRII), and platelet-derived growth factor receptors in WT/PyMT and AIB1$^{-/-}$/PyMT cell lines further and found no differences. Interestingly, among the five MMPs measured by qPCR, three of them (MMP1, MMP3, and MMP14) showed comparable expression levels, while two of them (MMP2 and MMP9) were expressed at much higher levels in WT/PyMT cells than in AIB1$^{-/-}$/PyMT cells (Fig. 4D and E and data not shown). The two AIB1$^{-/-}$/PyMT cell lines expressed very low levels of MMP2 and MMP9 mRNAs. The first WT/PyMT cell line expressed high levels of MMP9, and the second WT/PyMT cell line expressed even higher levels of MMP2 (Fig. 4D and E). In agreement with their mRNA expression patterns, IHC staining also revealed that WT/PyMT mammary tumor tissues had much higher levels of MMP2 and MMP9 proteins than did AIB1$^{-/-}$/PyMT mammary tumor tissues (Fig. 4F). In both WT/PyMT and AIB1$^{-/-}$/PyMT mammary tumors, MMP2 and MMP9 immunoreactivities were found to be located in the cell cytoplasm and the interstitial cellular matrix. However, in all five tumors examined for each group, both the number of immunostained cells and the intensity of overall MMP2 and MMP9 immunoreactivities were much higher in WT/PyMT tumors than in AIB1$^{-/-}$/PyMT tumors. Furthermore, WT/PyMT tumor cells also secreted more MMP2 or MMP9 enzyme activities into the culture medium than AIB1$^{-/-}$/PyMT cells, as measured by gelatin zymography assays (Fig. 4G). Semiquantitative measurements of three repeat assays by densitometry faithfully demonstrated that the two AIB1$^{-/-}$/PyMT cell lines secreted only low levels of MMP2 and MMP9 enzyme activities; the first WT/PyMT cell line secreted little MMP2 but a very high level of MMP9 activity, and the second WT/PyMT cell line secreted high levels of both MMP2 and MMP9 activities (Fig. 4H). These results suggest that AIB1 deficiency inhibits MMP2 and MMP9 expression and secretions in mammary tumors and cell lines.

AIB1 upregulates MMP2 and MMP9 expression in mouse and human breast cancer cells. If AIB1 is responsible for upregulating MMP2 and MMP9, the knockdown of AIB1 should reduce MMP2 and MMP9 expression in WT/PyMT cells accordingly. Indeed, when AIB1 mRNA and protein were significantly depleted in AIB1 siRNA-transfected WT/PyMT cells compared with scrambled control short double-stranded RNA (sdsRNA)-transfected WT/PyMT cells (Fig. 5A), the level of endogenous MMP2 mRNA expression was significantly reduced in the second WT/PyMT cell line that had a

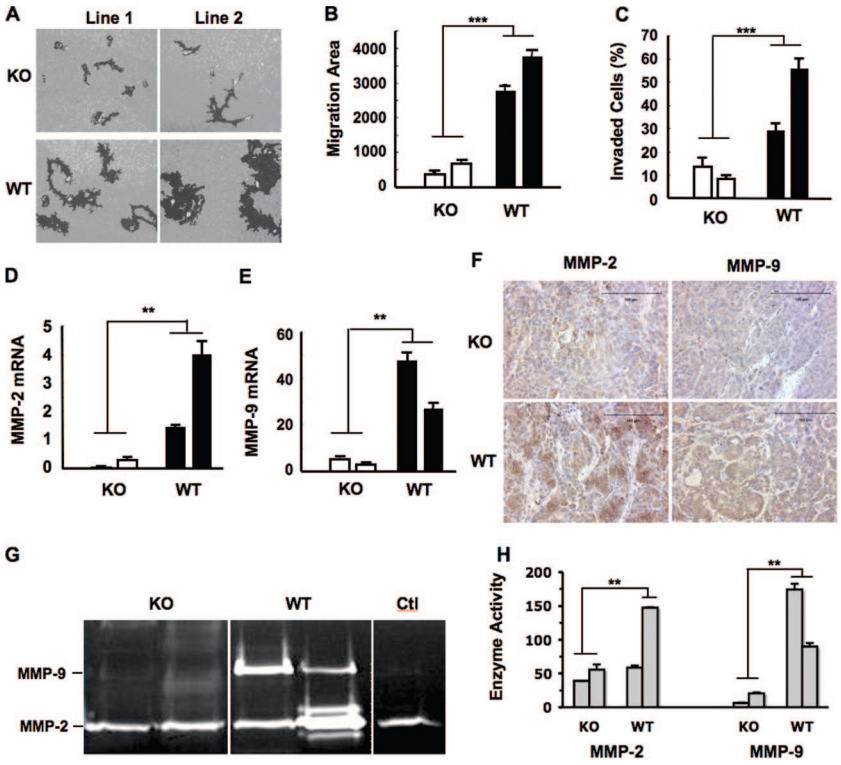

FIG. 4. AIB1 deficiency reduces mammary tumor cell migration, and invasion and inhibits MMP2 and MMP9 expression. (A) Images of cell migration tracks (black areas) for two AIB1$^{-/-}$ (KO)/PyMT and WT/PyMT cell lines. (B) Quantitative measurements of cell migration. The migration area of each cell was measured, and the average migration area for each cell line from 50 cells was calculated. ***, $P < 0.001$ by unpaired *t* test. (C) Cell invasion assay using Matrigel invasion chambers. Two lines of AIB1$^{-/-}$/PyMT (KO) and WT/PyMT (WT) cells were assayed. Data are presented as percentages of cells that invaded through the Matrigel layer for each cell line. ***, $P < 0.001$ by unpaired *t* test. (D and E) MMP2 and MMP9 mRNA levels in two AIB1$^{-/-}$/PyMT and WT/PyMT cell lines measured by qPCR. **, $P < 0.01$ by unpaired *t* test. (F) IHC for MMP2 and MMP9 in AIB1$^{-/-}$/PyMT and WT/PyMT mammary tumors with similar volumes. Tissues were counterstained with hematoxylin. (G) Gel images showing MMP2 and MMP9 activities measured by zymography assays. Conditioned media from two AIB1$^{-/-}$/PyMT and WT/PyMT cell lines were collected after 24 h of culture, and their loading volumes were normalized by measuring cellular protein amount. Medium in the culture dish without cells was used as a control (Ctl). (H) Average MMP2 and MMP9 enzyme activities quantified by densitometry from three repeat assays for each cell line. **, $P < 0.01$ by unpaired *t* test.

high level of MMP2 expression (Fig. 5B), and the level of MMP9 mRNA expression was also reduced significantly in both WT/PyMT cell lines (Fig. 5C). Accordingly, the knockdown of AIB1 in both lines of WT/PyMT cells caused a remarkable decrease in cell invasion in Matrigel-coated invasion assay chambers (Fig. 5D). These results demonstrate that the reduction of AIB1 in WT/PyMT cells inhibits MMP2 and MMP9 expression and cell invasion.

Conversely, if AIB1 deficiency is responsible for downregulating MMP2 and MMP9 expression in AIB1$^{-/-}$/PyMT cells, the restoration of AIB1 expression should accordingly increase MMP2 and MMP9 in these cells. In this experiment, human AIB1 was produced in AIB1$^{-/-}$/PyMT cells by adenoviral infection. Adenovirus-mediated GFP expression was used as a control (Fig. 5E). About 90% of cells were infected by the adenoviruses, as judged by GFP expression. As assayed by Western blotting, AIB1 protein levels in adenovirus-infected AIB1$^{-/-}$/PyMT cells were much higher than those in uninfected WT/PyMT cells (Fig. 5E). The expression of AIB1 significantly enhanced MMP9 expression in the first line of AIB1$^{-/-}$/PyMT cells and MMP2 expression in the second line of AIB1$^{-/-}$/PyMT cells (Fig. 5F and G), suggesting that AIB1 reexpression can enhance MMP2 and MMP9 expression levels in some but not all of these AIB1$^{-/-}$/PyMT cells. For unknown reasons, the expression levels of MMP2 and MMP9 in AIB1$^{-/-}$/PyMT cells with AIB1 restoration were still lower than those detected in WT/PyMT cells (Fig. 4D and E and 5F and G). Importantly, the restoration of AIB1 significantly promoted the invasive capabilities of AIB1$^{-/-}$/PyMT cells (Fig. 5H). Overall, these results demonstrate that AIB1 restoration in AIB1$^{-/-}$/PyMT cells can increase MMP2 or MMP9 expression and promote their invasive capabilities.

To investigate whether AIB1 also regulates MMP2 and MMP9 expression in human breast cancer cells, we transfected highly malignant MDA-MB-231 human breast cancer cells with either scrambled control sdsRNA or AIB1 siRNA and measured MMP2 and MMP9 mRNAs by qPCR. While AIB1 mRNA and protein were significantly reduced in siRNA-treated cells compared with sdsRNA-treated cells (Fig. 5I), the expression levels of MMP2 and MMP9 mRNAs dropped about 80% and 70%, respectively, in MDA-MB-231 cells with AIB1 knockdown (Fig. 5J and K). Decreases in MMP2 and MMP9 mRNAs were tightly associated with a significant decrease in the invasive behavior of MDA-MB-231 cells with AIB1 knock-

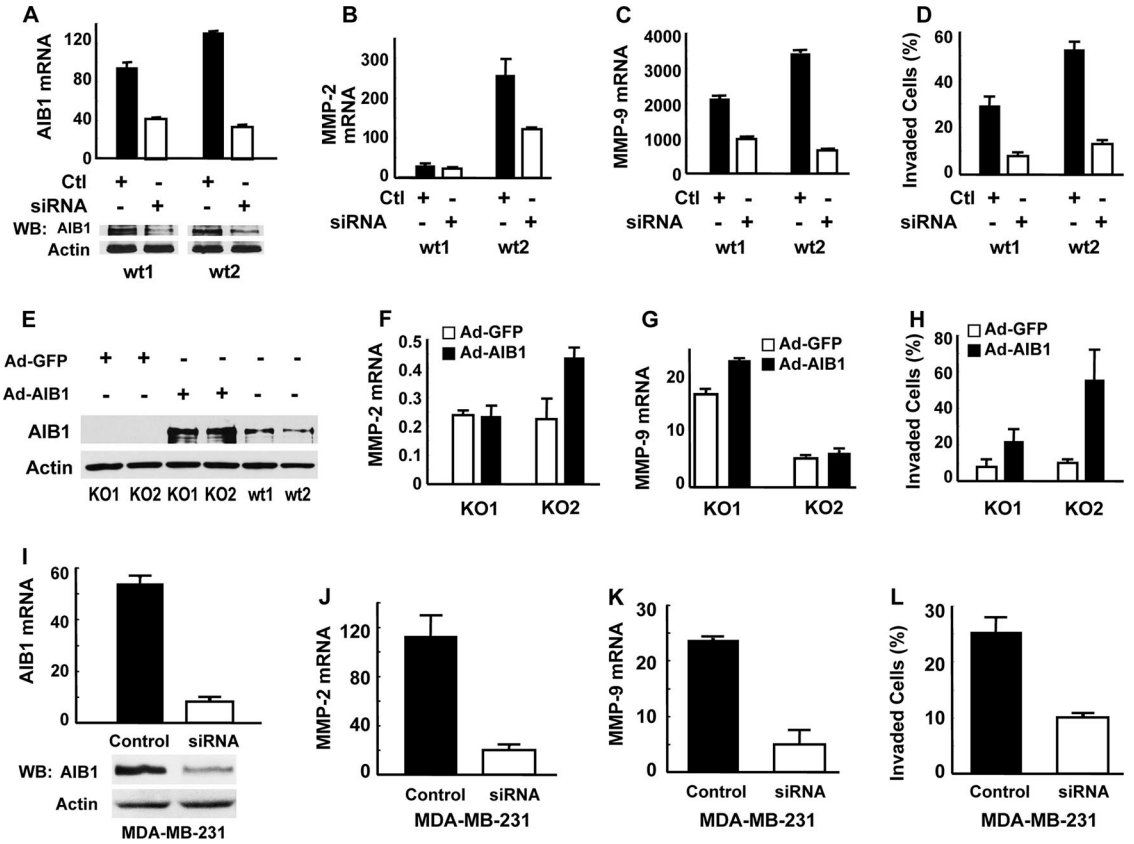

FIG. 5. AIB1 upregulates MMP2 and MMP9 expression and enhances cell invasion. (A) Knockdown of AIB1 in WT/PyMT cell lines (wt1 and wt2). Cells were transfected with control sdsRNA (Ctl) or siRNA specific to mouse AIB1 mRNA. Relative AIB1 mRNA levels were measured by qPCR. Protein levels were measured by Western blotting (WB). (B and C) AIB1 knockdown reduces MMP2 and MMP9 expression in WT/PyMT cell lines (wt1 and wt2). MMP2 and MMP9 mRNA levels were measured by qPCR after cells were transfected with AIB1 siRNA for 48 h. (D) AIB1 knockdown inhibits WT/PyMT cell invasion in the Matrigel invasion assay chamber. (E) Western blot for adenovirus-mediated AIB1 expression in AIB1$^{-/-}$/PyMT cell lines (KO1 and KO2). Adenoviral (Ad) expression of GFP and uninfected WT/PyMT cells served as negative and positive controls. (F and G) AIB1 expression in AIB1$^{-/-}$/PyMT cells partially increases MMP2 or MMP9 expression. MMP2 and MMP9 mRNA concentrations were measured by qPCR and normalized to endogenous 18S RNA. (H) AIB1 expression in AIB1$^{-/-}$/PyMT cells promotes cell invasion. (I) AIB1 knockdown by siRNA in human MDA-MB-231 cells. Cells were transfected with control sdsRNA or AIB1 siRNA. AIB1 mRNA and protein were measured by qPCR and Western blotting, respectively. (J and K) AIB1 knockdown in MDA-MB-231 cells reduces MMP2 and MMP9 expression. The expression levels of MMP2 and MMP9 mRNAs in AIB1 siRNA-treated cells were statistically lower ($P < 0.01$ by unpaired t test) than that in control sdsRNA-treated cells. (L) AIB1 knockdown in MDA-MB-231 cells inhibits cell invasion in a Matrigel invasion chamber.

down (Fig. 5L). These results indicate that AIB1 enhances MMP2 and MMP9 expression in both mouse mammary tumor and human metastatic breast cancer cells.

AIB1 coactivates PEA3-mediated activation of MMP2 and MMP9 promoters. To assess the mechanisms by which AIB1 regulates MMP2 and MMP9 expression, we performed transient transfection assays with transfection-susceptible HeLa cells using a pCR3.1-AIB1 expression vector and the previously described pGL3-MMP2-Luc and pGL3-MMP9-Luc promoter-luciferase reporter constructs (6, 21). Although HeLa cells contain endogenous AIB1 protein, the total level of AIB1 protein was increased in pCR3.1-AIB1-transfected cells in a dose-dependent manner (Fig. 6A and B). The levels of luciferase activities driven by the MMP2 and MMP9 promoters were also increased in an AIB1 dose-dependent manner, suggesting that AIB1 can enhance the activities of MMP2 and MMP9 promoters (Fig. 6A and B). Since c-Jun, NF-κB, and PEA3 are known transcription factors that can activate MMP2 and MMP9 promoters (5, 6, 21, 39), we further tested if AIB1 could coactivate any of these transcription factor-mediated MMP2 and MMP9 promoters. In the transfection assays, c-Jun expression had little effect on both MMP2 and MMP9 promoters. NF-κB or PEA3 expression increased MMP2 and MMP9 promoter activities by about twofold (Fig. 6C and D). While the coexpression of AIB1 was unable to coactivate either c-Jun- or NF-κB-mediated activation of MMP2 and MMP9 promoters, it promoted PEA3-mediated MMP2 and MMP9 promoter activities by about fourfold (Fig. 6C and D). Furthermore, the coexpression of AIB1 with PEA3 stimulated MMP2 and MMP9 promoter activities in an AIB1 dose-dependent manner (Fig. 6E). To address if AIB1 acts specifically on PEA3 over other Ets transcription factors, we replaced PEA3 with ERM or ER81 in transfection assays. We found that both ERM and ER81 enhanced MMP2 promoter activity in an AIB1-independent manner. However, AIB1 could promote ERM- and ER81-mediated MMP9 promoter activity

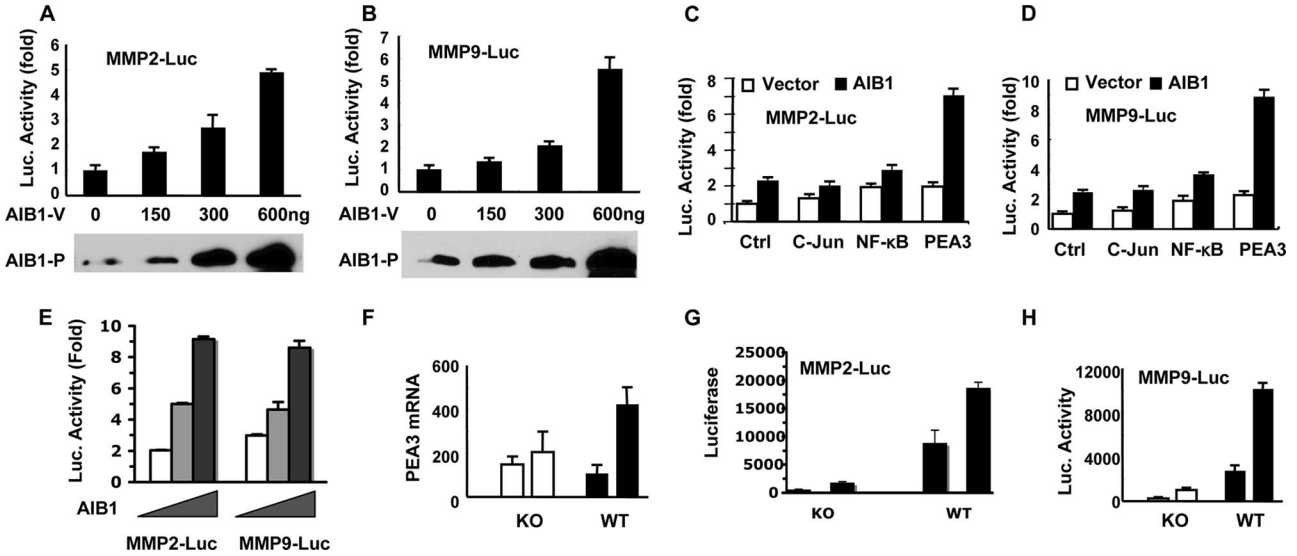

FIG. 6. AIB1 coactivates PEA3-mediated MMP2 and MMP9 promoter activities. (A and B) AIB1 activates MMP2 and MMP9 promoters in a dose-dependent manner. HeLa cells were transfected with MMP2-Luc or MMP9-Luc reporter DNA and different amounts of the AIB1 expression vector (AIB1-V) as indicated. AIB1 protein (AIB1-P) levels were examined by Western blotting with 50 μg total protein per lane. Luciferase activity was normalized to β-gal activity from a cotransfected β-gal expression vector. (C and D) PEA3 activates MMP2 and MMP9 promoters. HeLa cells were cotransfected with MMP2-Luc or MMP9-Luc reporter, parent vector (white bars), or AIB1 expression vector (black bars) and control (Ctrl), c-Jun, NF-κB, or PEA3 expression vectors as indicated. Luciferase activity was assayed 36 h after transfection. (E) AIB1 enhances PEA3-mediated MMP2 and MMP9 promoter activities in a dose-dependent manner. HeLa cells were transfected with 50 ng of PEA3 plasmids, 150 ng of MMP2-Luc or MMP9-Luc plasmids, and 0, 150, and 300 ng of AIB1 plasmids, respectively. Luciferase activity in 6 μg of total protein was assayed 36 h after transfection. (F) PEA3 mRNA levels in two AIB1$^{-/-}$/PyMT (KO) and WT/PyMT (WT) cell lines. One of the WT/PyMT cell lines expressed a higher level of PEA3 mRNA. (G and H) MMP2 and MMP9 promoter activities were much lower in AIB1$^{-/-}$/PyMT cell lines than in WT/PyMT cell lines. Cells were transfected with MMP2-Luc or MMP9-Luc plasmids and with the β-gal plasmids for the normalization of transfection efficiency.

(data not shown). These results suggest that AIB1 may increase MMP2 and MMP9 promoter activities by serving as a coactivator for PEA3 and certain other Ets family transcription factors.

To understand the functional relationships among PEA3, AIB1, and MMP2 and MMP9 expression in mammary tumor cells, we examined PEA3 expression and MMP2 and MMP9 promoter activities in AIB1$^{-/-}$/PyMT and WT/PyMT cell lines. PEA3 expression levels were not significantly different among the two AIB1$^{-/-}$/PyMT cell lines and the first WT/PyMT cell line, but its expression level was much higher in the second WT/PyMT cell line (Fig. 6F). When AIB1$^{-/-}$/PyMT and WT/PyMT cells were transfected with pGL3-MMP2-Luc and pGL3-MMP9-Luc under identical conditions, the MMP2 and MMP9 promoters exhibited much higher levels of activity in the two WT/PyMT cell lines than in the two AIB1$^{-/-}$/PyMT cell lines (Fig. 6G and H). In agreement with the higher level of PEA3 expression in the second WT/PyMT cell line, the MMP2 and MMP9 promoter activities were considerably higher in this cell line (Fig. 6G and H). These results demonstrate that the higher levels of PEA3 and AIB1 are associated with the higher levels of activity of MMP2 and MMP9 promoters in mammary tumor cells.

The AIB1 and PEA3 protein complexes directly associate with the MMP2 and MMP9 promoters. To investigate whether the MMP2 and MMP9 promoters were direct targets of PEA3 and AIB1, we performed co-IP and ChIP assays. The PEA3 protein was detected in WT/PyMT and AIB1$^{-/-}$/PyMT mouse mammary tumor cells and MDA-MB-231 human breast cancer cells. The AIB1 protein was detected in WT/PyMT and MDA-MB-231 cells but not in AIB1$^{-/-}$/PyMT cells, so AIB1$^{-/-}$/PyMT cells represent an ideal negative control in co-IP and ChIP experiments (Fig. 7A). AIB1 antibody coprecipitated AIB1 and PEA3 from the WT/PyMT cell lysates and nothing from AIB1$^{-/-}$/PyMT cell lysates. Reciprocally, PEA3 antibody coprecipitated PEA3 and AIB1 from the WT/PyMT cells but only PEA3 from the AIB1$^{-/-}$/PyMT cell lysates. Again, AIB1 or PEA3 antibodies, but not control IgG, also coprecipitated AIB1 and PEA3 from MDA-MB-231 cell lysates (Fig. 7A). These results indicate that AIB1 and PEA3 form protein complexes in mouse and human breast cancer cells.

Because the 5′-proximal regions of mouse and human MMP2 and MMP9 promoters contain multiple PEA3-binding sites, multiple pairs of PCR primers were designed for each promoter for ChIP assays (Table 1 and Fig. 7B to E). AIB1 antibody, but not control IgG, coprecipitated mMMP2 promoter DNA regions containing fragments B and C but not fragment A in ChIP assays using WT/PyMT mouse cells; this result was further validated by using AIB1$^{-/-}$/PyMT cells as negative controls (Fig. 7B). These results suggest that AIB1 is associated with regions B and C of the mMMP2 promoter. PEA3 antibody, but not control IgG, coprecipitated all (A, B, and C) fragments of the mMMP2 promoter, suggesting that PEA3 is associated with all three promoter regions (Fig. 7B). In the proximal region of the mMMP9 promoter, AIB1 antibody, but not control IgG, precipitated DNA fragments with a considerable amount of region B and a lesser amount of region A from WT/PyMT but not AIB1$^{-/-}$/PyMT (negative control)

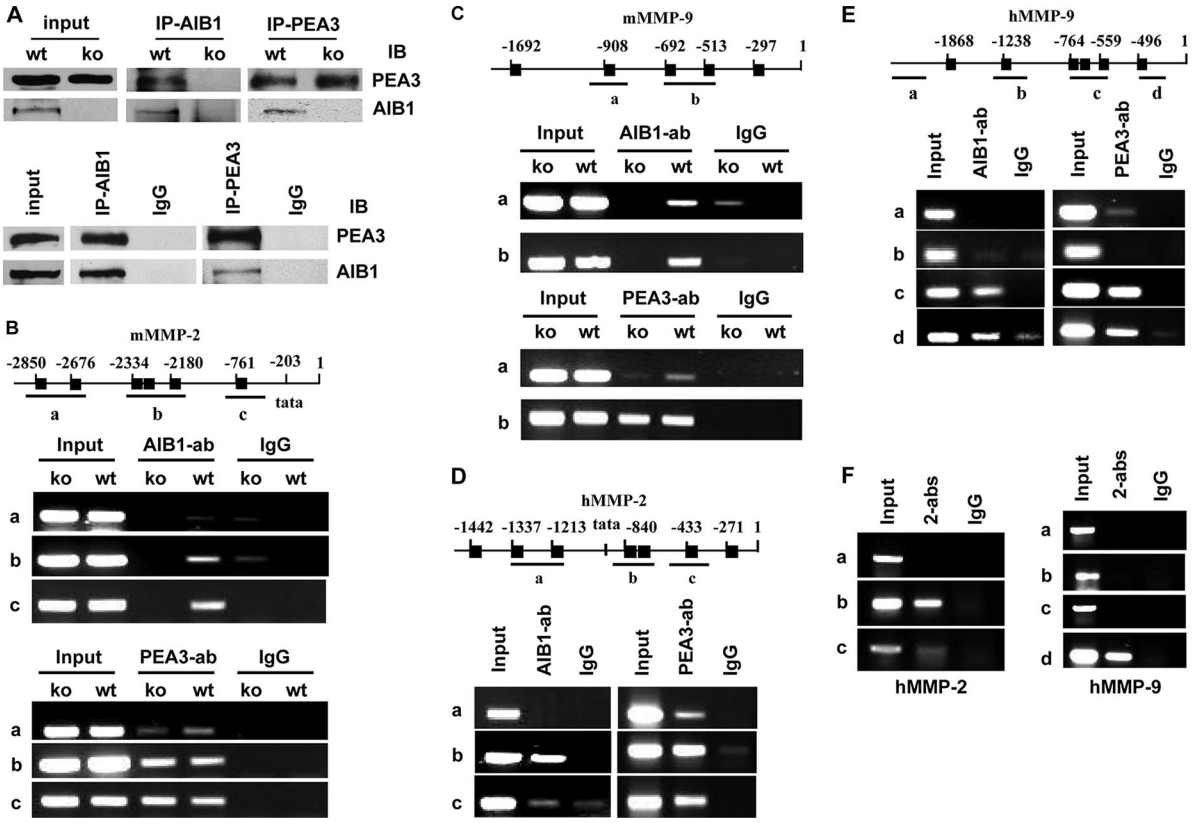

FIG. 7. AIB1 and PEA3 protein complexes are recruited for MMP2 and MMP9 promoters. (A) AIB1 and PEA3 form complexes. The lysates of WT/PyMT (wt) and AIB1$^{-/-}$/PyMT (ko) cells (top) as well as MDA-MB-231 cells (bottom) were subjected to co-IP (IP) with AIB1 and PEA3 antibodies. Immunoprecipitates were assayed by immunoblotting (IB) with PEA3 and AIB1 antibodies as indicated. Rabbit IgG was used as a negative control. The "input" lane represents 10% of cell lysate used for co-IP. (B) Association of AIB1 and PEA3 with the mMMP2 promoter. (Top) The mMMP2 promoter region contains six PEA3-binding sites (black boxes). Three primer pairs for regions A, B, and C were used in ChIP assays. (Middle) ChIP assays using AIB1$^{-/-}$/PyMT and WT/PyMT cells, AIB1 antibody, and control IgG. (Bottom) ChIP assays using AIB1$^{-/-}$/PyMT and WT/PyMT cells, PEA3 antibody, and IgG. Input lanes represent 5% of materials used for ChIP assays. (C) Association of AIB1 and PEA3 with the mMMP9 promoter. (Top) The mMMP9 promoter region contains five PEA3-binding sites. Two primer pairs were designed to detect regions A and B in ChIP assays. (Middle and bottom) ChIP assays using AIB1$^{-/-}$/PyMT and WT/PyMT cells, AIB1 and PEA3 antibodies, and control IgG. (D) Association of AIB1 and PEA3 with the hMMP2 promoter. (Top) The hMMP2 promoter region contains seven PEA3-binding sites. Three primer pairs were designed to detect regions A, B, and C in ChIP assays. (Bottom) ChIP assays using MDA-MB-231 cells, AIB1 and PEA3 antibodies, and control IgG. (E) Association of AIB1 and PEA3 with the hMMP9 promoter. (Top) The hMMP9 promoter region contains six PEA3-binding sites. Four primer pairs were used to detect regions A, B, C, and D in ChIP assays. (Bottom) ChIP assays using MDA-MB-231 cells, AIB1 and PEA3 antibodies, and control IgG. (F) ChIP-re-ChIP assays showing AIB1 and PEA3 protein complexes on hMMP2 and hMMP9 promoters. The first-step ChIP was performed with MDA-MB-231 cells, PEA3 antibody, and IgG. The second-step ChIP assays were performed with the eluates of first-step ChIP, AIB1 antibody (indicated as 2-abs), and IgG. PCR was performed to amply regions A to C of the hMMP2 promoter and regions A to D of the hMMP9 promoter.

cell samples. PEA3 antibody, but not control IgG, precipitated abundant region B but a lesser amount of region A from WT/PyMT and AIB1$^{-/-}$/PyMT cells (Fig. 7C). These results suggest that AIB1 and PEA3 are associated mainly with region B of the mMMP9 promoter, although lesser amounts of AIB1 and PEA3 are also associated with region A. In MDA-MB-231 human breast cancer cells, ChIP assays revealed that AIB1 was associated mainly with region B of the hMMP2 promoter and regions C and D of the hMMP9 promoter. PEA3 was associated with regions A, B, and C of the hMMP2 promoter and regions C and D of the hMMP9 promoter (Fig. 7D and E). These results indicate that AIB1 and PEA3 are associated with the MMP2 and MMP9 promoters not only in mouse mammary tumor cells but also in human breast cancer cells.

Next, ChIP-re-ChIP experiments were performed to address whether AIB1 and PEA3 formed protein-protein complexes on the MMP2 and MMP9 promoters in breast cancer cells. The eluted materials immunoprecipitated by the PEA3 antibody were resubjected to the second-step immunoprecipitation with AIB1 antibody by following an established protocol (44). Abundant fragment B and a lesser amount of fragment C of the hMMP2 promoter and abundant fragment D of the hMMP9 promoter were detected by PCR from the final immunoprecipitates (Fig. 7F). These results suggest that both AIB1 and PEA3 protein complexes are present on the hMMP2 and hMMP9 promoters.

Association of PEA3, AIB1, MMP2, and MMP9 expression in human breast tumors. Provoked by the above-described multiple lines of evidence demonstrating MMP2 and MMP9 upregulation by PEA3 and AIB1 in mouse mammary tumors

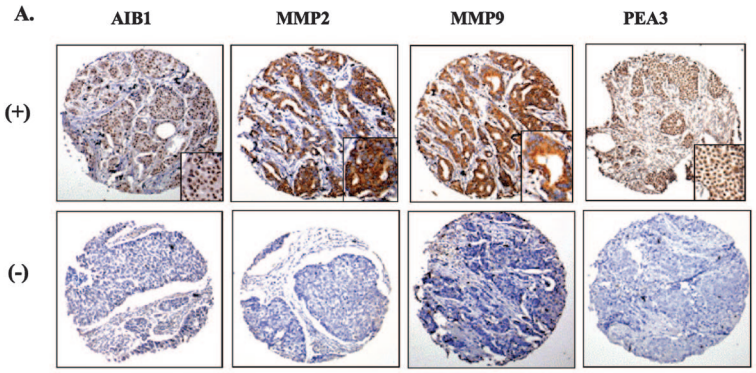

B. Associations of AIB1, MMP2, MMP9 and PEA3 expression

	Total=560	AIB1 +	P-value	MMP2+	P-value	MMP9+	p-value	PEA3+	P-value
AIB1 + AIB1 -	73.8% 26.2%			76.4% 23.6%	<0.001	76.1% 23.9%	0.004	85.4% 14.6%	<0.001
MMP2 + MMP2 -	91.3% 8.7%	95.5% 4.5%	<0.001			94.4% 5.6%	<0.0000 1	93.4% 6.6%	0.0158
MMP9 + MMP9 -	88.5% 11.5%	91.8% 8.2%	0.004	92.9% 7.1%	<0.00001			94.3% 5.7%	0.0078
PEA3 + PEA3 -	53.1% 46.9%	44.2% 55.8%	<0.001	53.4% 46.6%	0.0158	54.6% 45.4%	0.0078		

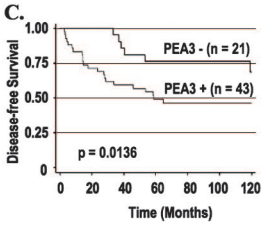

FIG. 8. Association of AIB1, PEA3, MMP2, and MMP9 expression in human breast tumors. (A) Representative immunohistochemical staining of breast tumor arrays positive (+) and negative (−) for AIB1, MMP2, MMP9, and PEA3. One area of the photograph is shown at a higher magnification in the lower right corner of each panel. (B) Associated expression of AIB1, MMP2, MMP9, and PEA3 in 560 human breast tumors. Statistical analysis was performed using the Fisher's exact test, and a P value of <0.05 is considered to be significant. (C) Kaplan-Meier estimates of DFS of breast cancer patients according to PEA3 expression in a HER2-positive population. The indicated P value was calculated by Wilcoxon test.

and human breast cancer cell lines, we next analyzed the expression profiles of PEA3, AIB1, MMP2, and MMP9 in 560 human breast tumors by IHC. The immunoreactivities of PEA3 and AIB1 were observed predominantly in the nuclei, while MMP2 and MMP9 were observed in the cytosol and extracellular matrix of breast tumor cells (Fig. 8A). Among all tumors examined, 74% of them were AIB1 positive. About 76% of AIB1-positive tumors were MMP2 and MMP9 positive, and 85% of AIB1-positive tumors were PEA3 positive (Fig. 8B). Furthermore, 96% and 93% of MMP2-positive tumors were found to be positive for anti-AIB1 and anti-PEA3 staining. Similarly, 92% and 94% of MMP9-positive tumors were found to be positive for AIB1 and PEA3, respectively (Fig. 8B). Statistical analyses indicate that the associations between AIB1 and MMP2, MMP9, and PEA3 expressions are significant ($P < 0.001$, $P = 0.004$, and $P < 0.001$, respectively). The associations of PEA3 expression with MMP2 and MMP9 expression are significant ($P = 0.016$ and $P = 0.008$, respectively). Finally, a significant association between MMP2 and MMP9 expressions was also observed in breast tumors ($P < 0.00001$) (Fig. 8B). The combined results substantiate that the expression profiles of AIB1, PEA3, MMP2, and MMP9 are positively correlated, supporting the notion that AIB1 is a coactivator that promotes PEA3-mediated MMP2 and MMP9 expression in breast tumor cells.

Clinical pathological parameters were further analyzed in relation to the expression of AIB1, PEA3, MMP2, and MMP9. Although none of the variables analyzed independently predicted disease-free survival (DFS), in either the tamoxifen-treated or untreated populations, PEA3 was found to be a strong predictor of reduced DFS in HER2-positive breast cancer patients ($P = 0.0136$ by Wilcoxon test) (Fig. 8C).

DISCUSSION

We previously showed that the disruption of AIB1 suppressed v-Ha-ras and chemical carcinogen 7,12-dimethylbenz-[a]anthracene-induced mammary tumorigenesis (24, 25). Because of the low rates and big variations of metastasis in these models, the genetic role of AIB1 in breast cancer metastasis has not been assessed in vivo. In this study, our data reveal that AIB1 deficiency extends the latency of PyMT-induced mammary tumorigenesis, a result that is consistent with our previous models. Most importantly, this study now demonstrates that the genetic ablation of AIB1 reduces lung metastasis in AIB1$^{-/-}$/PyMT mice and recipient mice bearing transplanted AIB1$^{-/-}$/PyMT tumors compared with the tumorigenic latency and metastatic extent in WT/PyMT mice and recipient mice bearing transplanted WT/PyMT tumors of comparable size. During tumor progression, WT tumor cells undergo EMT characteristics of the reduction or loss of epithelial markers such as E-cadherin, β-catenin, ZO-1, and CK8 and gain of mesenchymal markers such as N-cadherin and vimentin. Consequently, WT tumor cells cannot form differentiated and polarized epithelial structures in a 3D culture system. Instead, they form a disorganized and highly invasive cellular mass in Matrigel. In contrast, AIB1$^{-/-}$ tumor cells are able to maintain their E-cadherin, ZO-1, and CK8 expression levels, largely suppress N-cadherin and vimentin expression, and form differentiated and polarized acinar structures in the 3D culture system.

These results suggest that AIB1 plays an important role in the promotion of EMT during breast cancer progression in mice.

EMT, where cells change from a polarized, epithelial phenotype to a highly motile fibroblastoid or mesenchymal phenotype, is a central process during breast cancer progression to invasive and metastatic stages. Our data show that WT/PyMT tumor cells with an EMT phenotype exhibit fast migration on culture plates and rapid invasion through Matrigel that simulates the extracellular matrix (ECM). In contrast, AIB1$^{-/-}$/PyMT tumor cells with a limited EMT phenotype migrate and invade much slower than WT/PyMT tumor cells. Since the motility and invasiveness of cancer cells positively correlate with their metastatic capability, it is logical that the observed decrease in cell migration and invasion should be responsible, at least in part, for the reduced lung metastasis of AIB1$^{-/-}$ mammary tumors in mice.

MMPs are among the known factors that promote tumor cell motility, invasiveness, and EMT. MMPs degrade the dense ECM molecules including laminin, collagens, fibronectin, and proteoglycans to create space for tumor cells to move, and they activate certain growth factors associated with the ECM or cell surfaces (50). Furthermore, the ectopic expression of MMP-3 is sufficient to drive mammary epithelial cells through all steps of tumorigenesis including the invasion-metastasis cascade, although the molecular mechanism is not clear (42). In this study, multiple lines of evidence confirmed that AIB1 plays a crucial role in the upregulation of MMP2 and MMP9 in mammary tumor cells. First, levels of the MMP2 and MMP9 mRNAs, proteins, and enzyme activities in WT tumor cells were significantly higher than those in AIB1$^{-/-}$ tumor cells, suggesting that AIB1 is required for MMP2 and MMP9 expression in breast tumor cells; second, AIB1 knockdown in both WT mouse tumor cells and human breast cancer cells greatly reduced MMP2 and MMP9 expression and cell-invasive behavior; and third, AIB1 restoration in AIB1$^{-/-}$ tumor cells successfully increased MMP2 and MMP9 expression and cell-invasive behavior. Collectively, these new data indicate that AIB1 is involved in the upregulation of MMP2 and MMP9 in breast cancer.

We addressed how AIB1 regulates the expression of MMP2 and MMP9. In our animal model, PyMT induces mammary tumorigenesis and lung metastasis through the activation of Shc–Ras–mitogen-activated protein kinase (MAPK) and c-Src–phosphatidylinositol-3 kinase–Akt pathways that are normally stimulated by receptor tyrosine kinases (12). The major downstream effectors of the MAPK pathway include the Ets and AP-1 transcription factors that enhance MMP2 and MMP9 expression (12). In addition to the binding sites for AP-1 and the Ets family member PEA3, the proximal regions of the MMP2 and MMP9 promoters contain putative NF-κB binding sites (5, 7, 21, 40). Since studies using cultured cells have characterized AIB1 as being a coactivator for PEA3, AP-1, and NF-κB (18, 51, 56), we hypothesized that AIB1 deficiency could decrease the functions of these transcription factors and restrict MMP2 and MMP9 overexpression in tumor cells. Interestingly, our data demonstrated that AIB1 enhanced MMP2 and MMP9 promoter activities in a dose-dependent manner; AIB1 selectively coactivated the PEA3-mediated expression of the two MMP promoters but exerted little coactivation for c-Jun and NF-κB on these two promoters. This is consistent with our previous study showing that the mRNAs of proinflammatory cytokines, a group of NF-κB and AP-1 target genes, were comparably transcribed in activated WT and AIB1$^{-/-}$ macrophages, suggesting that AIB1 is a physiological coactivator for NF-κB and AP-1 only in certain cell types (58). Our results further confirmed that AIB1 and PEA3 formed complexes in both mouse and human breast cancer cells, and these protein complexes were associated together at the proximal MMP2 and MMP9 promoter regions containing PEA3 binding sites. ChIP assays detected that PEA3 was associated with all examined fragments of mMMP2 and mMMP9 promoters in both WT/PyMT and AIB1$^{-/-}$/PyMT cells, suggesting that AIB1 is not required for PEA3 to bind to DNA. Interestingly, most but not all of the DNA fragments associated with PEA3 were found to be associated with AIB1. For example, fragments A, B, and C of mMMP2 and hMMP2 promoters are associated with PEA3, while only fragments B and C are associated with AIB1. On the other hand, although ChIP assays revealed that both PEA3 and AIB1 were associated with fragments C and D of the hMMP9 promoter, ChIP-re-ChIP assays could detect only fragment D associated with both PEA3 and AIB1. These results suggest that AIB1 may not be recruited to all PEA3-binding sites of MMP2 and MMP9 promoters, and AIB1 also can be recruited to these promoters by other as-yet-unidentified transcription factors. Taken together, these findings indicate that the MMP2 and MMP9 promoters are direct targets of PEA3 and AIB1. In addition, AIB1 may also coactivate certain other Ets family members such as ERM and ER81 to enhance MMP9 expression.

It is conceivable that AIB1 may also promote breast cancer metastasis through other pathways. Previous studies showed that AIB1 is required for the EGF-induced activation of EGF receptor and HER2 (27) and for the full activation of the IGF-I signaling pathway (25, 47); HER2- and v-Ha-ras-induced mammary tumorigenesis is blocked or delayed in AIB1$^{-/-}$ mice (15, 25), and AIB1 activity and concentrations can be modulated by posttranslational modifications such as phosphorylation and ubiquitination controlled by growth factors, cytokines, and hormones (52, 53, 59). Since these pathways also contribute to breast cancer metastasis, the reduction of AIB1$^{-/-}$/PyMT tumor cell metastasis may be attributed to a combined effect on multiple signaling pathways that involve AIB1.

Previous studies independently examined the expression of PEA3, AIB1, MMP2, and MMP9 in breast cancers. PEA3 is upregulated in both human and mouse metastatic adenocarcinomas (4, 22, 48). In human breast cancer, PEA3 expression is positively correlated with HER2 expression, tumor grade, reduced DFS, and axillary lymph node metastasis (33, 34). The inhibition of PEA3 can suppress HER2/Neu-induced mammary tumorigenesis in mice (41). AIB1 is amplified and overexpressed in a subgroup of breast tumors, and its overexpression is positively correlated with HER2 expression (1, 33, 34, 37). In addition, AIB1 is colocalized with PEA3 in the nuclei of invasive breast carcinoma cells (17). MMPs are upregulated in most human and animal tumors as well as in most tumor cell lines. Changes in MMP levels can markedly affect the invasive behavior of tumor cells and their ability to metastasize in animal models (31). In certain cases, the stage of cancer progression is positively correlated with the expression of MMP

family members including MMP2 and MMP9 (43). In breast cancer, MMP2 and MMP9 appear to promote tumor initiation, invasion, and metastasis (13). Since our data demonstrated that AIB1 serves as a coactivator for PEA3 to enhance MMP2 and MMP9 expression in both mouse and human breast cancer cells, we reasoned that levels of all four of these proteins would be associated in human breast tumors. Indeed, after examining a large cohort of 560 breast tumors, we found that the protein levels of AIB1, PEA3, MMP2, and MMP9 were positively correlated in these tumor samples. These results are consistent with our results from mouse models and human breast cancer cell lines, validating the important role of AIB1 in the PEA3-mediated upregulation of MMP2 and MMP9 and the inevitable contribution of the MAPK-PEA3-AIB1-MMP2/MMP9 pathway in breast cancer initiation and progression.

Interestingly, PEA3, AIB1, MMP2, and MMP9 were undetectable by IHC in normal breast tissues and some breast tumor samples. However, the PEA3, AIB1, MMP2, and MMP9 proteins were detected in 53%, 74%, 91%, and 89% of breast tumors, respectively. The higher expression rates of MMP2 and MMP9 than those of PEA3 and AIB1 may be partially explained by experimental data showing that an increase in either PEA3 or AIB1 alone could enhance MMP2 and MMP9 promoter activities. Additionally, some unknown transcription factors that regulate MMP2 and MMP9 expression may also be upregulated in some of the breast tumors. It was previously reported that AIB1 levels detected by Western blotting could be an independent poor prognostic factor in tamoxifen-treated HER2-positive patients (37). In contrast, in this study, the variables examined in a cohort of 560 patients by IHC did not prove to be significant indicators of the recurrence of disease in treated or untreated patient populations. However, in line with previously reported observations, in the HER2/Neu-positive population, PEA3 expression was found to be a predictor of reduced DFS, indicating a strong relationship between these two proteins in breast cancer progression in the clinical setting (34).

In summary, we have demonstrated that MMP2 and MMP9 are target genes of PEA3/AIB1-mediated transcription. AIB1 expressed in mouse and human breast cancers plays an inevitable role in upregulating MMP2 and MMP9 and promoting tumor cell invasion and metastasis. Consequently, the knockout (KO) or knockdown of AIB1 in mouse or human breast cancer cells inhibits MMP2 and MMP9 expression and reduces tumor cell-invasive and metastatic capabilities. This study highlights a potential intervention point for the control of breast cancer by targeting the PEA3/AIB1 pathway to inhibit the expression of MMP2 and MMP9. It is especially significant in the situation that current MMP inhibitors have been ineffective in clinical trials due to severe side effects and an insufficient number of specific inhibitors of individual MMPs (10).

ACKNOWLEDGMENTS

We thank Ralf Janknecht, Xin Lin, Sun Yi, and Ping Yi for PEA3, NF-κB, MMP2-Luc, and AP-1 plasmids and Junjiang Fu and Brian York for experimental assistance.

This work is partially supported by National Institutes of Health grants CA112403 and CA119689 to J.X. and DK59820 and HD07857 to B.W.O. and American Cancer Society Scholar Award RSG-05-082-01-TBE to J.X. L.Q. is a recipient of a Susan Komen Breast Cancer postdoctoral fellowship.

REFERENCES

1. **Anzick, S. L., J. Kononen, R. L. Walker, D. O. Azorsa, M. M. Tanner, X. Y. Guan, G. Sauter, O. P. Kallioniemi, J. M. Trent, and P. S. Meltzer.** 1997. AIB1, a steroid receptor coactivator amplified in breast and ovarian cancer. Science **277:**965–968.
2. **Bai, J., Y. Uehara, and D. J. Montell.** 2000. Regulation of invasive cell behavior by taiman, a Drosophila protein related to AIB1, a steroid receptor coactivator amplified in breast cancer. Cell **103:**1047–1058.
3. **Bautista, S., H. Valles, R. L. Walker, S. Anzick, R. Zeillinger, P. Meltzer, and C. Theillet.** 1998. In breast cancer, amplification of the steroid receptor coactivator gene AIB1 is correlated with estrogen and progesterone receptor positivity. Clin. Cancer Res. **4:**2925–2929.
4. **Benz, C. C., R. C. O'Hagan, B. Richter, G. K. Scott, C. H. Chang, X. Xiong, K. Chew, B. M. Ljung, S. Edgerton, A. Thor, and J. A. Hassell.** 1997. HER2/Neu and the Ets transcription activator PEA3 are coordinately upregulated in human breast cancer. Oncogene **15:**1513–1525.
5. **Bergman, M. R., S. Cheng, N. Honbo, L. Piacentini, J. S. Karliner, and D. H. Lovett.** 2003. A functional activating protein 1 (AP-1) site regulates matrix metalloproteinase 2 (MMP-2) transcription by cardiac cells through interactions with JunB-Fra1 and JunB-FosB heterodimers. Biochem. J. **369:**485–496.
6. **Bian, J., and Y. Sun.** 1997. Transcriptional activation by p53 of the human type IV collagenase (gelatinase A or matrix metalloproteinase 2) promoter. Mol. Cell. Biol. **17:**6330–6338.
7. **Borden, P., and R. A. Heller.** 1997. Transcriptional control of matrix metalloproteinases and the tissue inhibitors of matrix metalloproteinases. Crit. Rev. Eukaryot. Gene Expr. **7:**159–178.
8. **Chen, H., R. J. Lin, R. L. Schiltz, D. Chakravarti, A. Nash, L. Nagy, M. L. Privalsky, Y. Nakatani, and R. M. Evans.** 1997. Nuclear receptor coactivator ACTR is a novel histone acetyltransferase and forms a multimeric activation complex with P/CAF and CBP/p300. Cell **90:**569–580.
9. **Chung, A. C., S. Zhou, L. Liao, J. C. Tien, N. M. Greenberg, and J. Xu.** 2007. Genetic ablation of the amplified-in-breast cancer 1 inhibits spontaneous prostate cancer progression in mice. Cancer Res. **67:**5965–5975.
10. **Coussens, L. M., B. Fingleton, and L. M. Matrisian.** 2002. Matrix metalloproteinase inhibitors and cancer: trials and tribulations. Science **295:**2387–2392.
11. **Debnath, J., S. K. Muthuswamy, and J. S. Brugge.** 2003. Morphogenesis and oncogenesis of MCF-10A mammary epithelial acini grown in three-dimensional basement membrane cultures. Methods **30:**256–268.
12. **Dennis, J. W., M. Granovsky, and C. E. Warren.** 1999. Glycoprotein glycosylation and cancer progression. Biochim. Biophys. Acta **1473:**21–34.
13. **Duffy, M. J., T. M. Maguire, A. Hill, E. McDermott, and N. O'Higgins.** 2000. Metalloproteinases: role in breast carcinogenesis, invasion and metastasis. Breast Cancer Res. **2**:252–257.
14. **Feng, Q., P. Yi, J. Wong, and B. W. O'Malley.** 2006. Signaling within a coactivator complex: methylation of SRC-3/AIB1 is a molecular switch for complex disassembly. Mol. Cell. Biol. **26:**7846–7857.
15. **Fereshteh, M. P., M. T. Tilli, S. E. Kim, J. Xu, B. W. O'Malley, A. Wellstein, P. A. Furth, and A. T. Riegel.** 2008. The nuclear receptor coactivator amplified in breast cancer-1 is required for Neu (ErbB2/HER2) activation, signaling, and mammary tumorigenesis in mice. Cancer Res. **68:**3697–3706.
16. **Fisher, S. J., and Z. Werb.** 1995. The catabolism of extracellular matrix. IRL Press, Oxford, United Kingdom.
17. **Fleming, F. J., E. Myers, G. Kelly, T. B. Crotty, E. W. McDermott, N. J. O'Higgins, A. D. Hill, and L. S. Young.** 2004. Expression of SRC-1, AIB1, and PEA3 in HER2 mediated endocrine resistant breast cancer; a predictive role for SRC-1. J. Clin. Pathol. **57:**1069–1074.
18. **Goel, A., and R. Janknecht.** 2004. Concerted activation of ETS protein ER81 by p160 coactivators, the acetyltransferase p300 and the receptor tyrosine kinase HER2/Neu. J. Biol. Chem. **279:**14909–14916.
19. **Guan, X. Y., J. Xu, S. L. Anzick, H. Zhang, J. M. Trent, and P. S. Meltzer.** 1996. Hybrid selection of transcribed sequences from microdissected DNA: isolation of genes within amplified region at 20q11-q13.2 in breast cancer. Cancer Res. **56:**3446–3450.
20. **Guy, C. T., R. D. Cardiff, and W. J. Muller.** 1992. Induction of mammary tumors by expression of polyomavirus middle T oncogene: a transgenic mouse model for metastatic disease. Mol. Cell. Biol. **12:**954–961.
21. **Hah, N., and S. T. Lee.** 2003. An absolute role of the PKC-dependent NF-kappaB activation for induction of MMP-9 in hepatocellular carcinoma cells. Biochem. Biophys. Res. Commun. **305:**428–433.
22. **Hesselbrock, D. R., N. Kurpios, J. A. Hassell, M. A. Watson, and T. P. Fleming.** 2005. PEA3, AP-1, and a unique repetitive sequence all are involved in transcriptional regulation of the breast cancer-associated gene, mammaglobin. Breast Cancer Res. Treat. **89:**289–296.
23. **Itoh, M., A. Nagafuchi, S. Yonemura, T. Kitani-Yasuda, S. Tsukita, and S. Tsukita.** 1993. The 220-kD protein colocalizing with cadherins in non-epithelial cells is identical to ZO-1, a tight junction-associated protein in epithelial cells: cDNA cloning and immunoelectron microscopy. J. Cell Biol. **121:**491–502.
24. **Kuang, S. Q., L. Liao, S. Wang, D. Medina, B. W. O'Malley, and J. Xu.** 2005.

Mice lacking the amplified in breast cancer 1/steroid receptor coactivator-3 are resistant to chemical carcinogen-induced mammary tumorigenesis. Cancer Res. **65:**7993–8002.
25. **Kuang, S. Q., L. Liao, H. Zhang, A. V. Lee, B. W. O'Malley, and J. Xu.** 2004. AIB1/SRC-3 deficiency affects insulin-like growth factor I signaling pathway and suppresses v-Ha-ras-induced breast cancer initiation and progression in mice. Cancer Res. **64:**1875–1885.
26. **Kuang, S. Q., L. Liao, H. Zhang, F. A. Pereira, Y. Yuan, F. J. DeMayo, L. Ko, and J. Xu.** 2002. Deletion of the cancer-amplified coactivator AIB3 results in defective placentation and embryonic lethality. J. Biol. Chem. **277:**45356–45360.
27. **Lahusen, T., M. Fereshteh, A. Oh, A. Wellstein, and A. T. Riegel.** 2007. Epidermal growth factor receptor tyrosine phosphorylation and signaling controlled by a nuclear receptor coactivator, amplified in breast cancer 1. Cancer Res. **67:**7256–7265.
28. **List, H. J., K. J. Lauritsen, R. Reiter, C. Powers, A. Wellstein, and A. T. Riegel.** 2001. Ribozyme targeting demonstrates that the nuclear receptor coactivator AIB1 is a rate-limiting factor for estrogen-dependent growth of human MCF-7 breast cancer cells. J. Biol. Chem. **276:**23763–23768.
29. **List, H. J., R. Reiter, B. Singh, A. Wellstein, and A. T. Riegel.** 2001. Expression of the nuclear coactivator AIB1 in normal and malignant breast tissue. Breast Cancer Res. Treat. **68:**21–28.
30. **Louie, M. C., A. S. Revenko, J. X. Zou, J. Yao, and H. W. Chen.** 2006. Direct control of cell cycle gene expression by proto-oncogene product ACTR, and its autoregulation underlies its transforming activity. Mol. Cell. Biol. **26:**3810–3823.
31. **McCawley, L. J., and L. M. Matrisian.** 2000. Matrix metalloproteinases: multifunctional contributors to tumor progression. Mol. Med. Today **6:**149–156.
32. **Mussi, P., C. Yu, B. W. O'Malley, and J. Xu.** 2006. Stimulation of steroid receptor coactivator-3 (SRC-3) gene overexpression by a positive regulatory loop of E2F1 and SRC-3. Mol. Endocrinol. **20:**3105–3119.
33. **Myers, E., A. D. Hill, G. Kelly, E. W. McDermott, N. J. O'Higgins, Y. Buggy, and L. S. Young.** 2005. Associations and interactions between Ets-1 and Ets-2 and coregulatory proteins, SRC-1, AIB1, and NCoR in breast cancer. Clin. Cancer Res. **11:**2111–2122.
34. **Myers, E., A. D. Hill, G. Kelly, E. W. McDermott, N. J. O'Higgins, and L. S. Young.** 2006. A positive role for PEA3 in HER2-mediated breast tumour progression. Br. J. Cancer **95:**1404–1409.
35. **Norton, P. A., and J. M. Coffin.** 1985. Bacterial β-galactosidase as a marker of Rous sarcoma virus gene expression and replication. Mol. Cell. Biol. **5:**281–290.
36. **Onate, S. A., S. Y. Tsai, M. J. Tsai, and B. W. O'Malley.** 1995. Sequence and characterization of a coactivator for the steroid hormone receptor superfamily. Science **270:**1354–1357.
37. **Osborne, C. K., V. Bardou, T. A. Hopp, G. C. Chamness, S. G. Hilsenbeck, S. A. Fuqua, J. Wong, D. C. Allred, G. M. Clark, and R. Schiff.** 2003. Role of the estrogen receptor coactivator AIB1 (SRC-3) and HER-2/neu in tamoxifen resistance in breast cancer. J. Natl. Cancer Inst. **95:**353–361.
38. **Planas-Silva, M. D., Y. Shang, J. L. Donaher, M. Brown, and R. A. Weinberg.** 2001. AIB1 enhances estrogen-dependent induction of cyclin D1 expression. Cancer Res. **61:**3858–3862.
39. **Sanceau, J., D. D. Boyd, M. Seiki, and B. Bauvois.** 2002. Interferons inhibit tumor necrosis factor-alpha-mediated matrix metalloproteinase-9 activation via interferon regulatory factor-1 binding competition with NF-kappa B. J. Biol. Chem. **277:**35766–35775.
40. **Sato, H., and M. Seiki.** 1993. Regulatory mechanism of 92 kDa type IV collagenase gene expression which is associated with invasiveness of tumor cells. Oncogene **8:**395–405.
41. **Shepherd, T. G., L. Kockeritz, M. R. Szrajber, W. J. Muller, and J. A. Hassell.** 2001. The pea3 subfamily ets genes are required for HER2/Neu-mediated mammary oncogenesis. Curr. Biol. **11:**1739–1748.
42. **Sternlicht, M. D., A. Lochter, C. J. Sympson, B. Huey, J. P. Rougier, J. W. Gray, D. Pinkel, M. J. Bissell, and Z. Werb.** 1999. The stromal proteinase MMP3/stromelysin-1 promotes mammary carcinogenesis. Cell **98:**137–146.
43. **Stetler-Stevenson, W. G.** 1996. Dynamics of matrix turnover during pathologic remodeling of the extracellular matrix. Am. J. Pathol. **148:**1345–1350.
44. **Stewart, M. D., J. Li, and J. Wong.** 2005. Relationship between histone H3 lysine 9 methylation, transcription repression, and heterochromatin protein 1 recruitment. Mol. Cell. Biol. **25:**2525–2538.
45. **Tilli, M. T., R. Reiter, A. S. Oh, R. T. Henke, K. McDonnell, G. I. Gallicano, P. A. Furth, and A. T. Riegel.** 2005. Overexpression of an N-terminally truncated isoform of the nuclear receptor coactivator amplified in breast cancer 1 leads to altered proliferation of mammary epithelial cells in transgenic mice. Mol. Endocrinol. **19:**644–656.
46. **Torchia, J., D. W. Rose, J. Inostroza, Y. Kamei, S. Westin, C. K. Glass, and M. G. Rosenfeld.** 1997. The transcriptional co-activator p/CIP binds CBP and mediates nuclear-receptor function. Nature **387:**677–684.
47. **Torres-Arzayus, M. I., J. F. De Mora, J. Yuan, F. Vazquez, R. Bronson, M. Rue, W. R. Sellers, and M. Brown.** 2004. High tumor incidence and activation of the PI3K/AKT pathway in transgenic mice define AIB1 as an oncogene. Cancer Cell **6:**263–274.
48. **Trimble, M. S., J. H. Xin, C. T. Guy, W. J. Muller, and J. A. Hassell.** 1993. PEA3 is overexpressed in mouse metastatic mammary adenocarcinomas. Oncogene **8:**3037–3042.
49. **Wang, Z., D. W. Rose, O. Hermanson, F. Liu, T. Herman, W. Wu, D. Szeto, A. Gleiberman, A. Krones, K. Pratt, R. Rosenfeld, C. K. Glass, and M. G. Rosenfeld.** 2000. Regulation of somatic growth by the p160 coactivator p/CIP. Proc. Natl. Acad. Sci. USA **97:**13549–13554.
50. **Weinberg, R. A.** 2007. The biology of cancer. Garland Science, Taylor & Francis Group, New York, NY.
51. **Werbajh, S., I. Nojek, R. Lanz, and M. A. Costas.** 2000. RAC-3 is a NF-kappa B coactivator. FEBS Lett. **485:**195–199.
52. **Wu, R. C., Q. Feng, D. M. Lonard, and B. W. O'Malley.** 2007. SRC-3 coactivator functional lifetime is regulated by a phospho-dependent ubiquitin time clock. Cell **129:**1125–1140.
53. **Wu, R. C., J. Qin, P. Yi, J. Wong, S. Y. Tsai, M. J. Tsai, and B. W. O'Malley.** 2004. Selective phosphorylations of the SRC-3/AIB1 coactivator integrate genomic responses to multiple cellular signaling pathways. Mol. Cell **15:**937–949.
54. **Xu, J., and Q. Li.** 2003. Review of the in vivo functions of the p160 steroid receptor coactivator family. Mol. Endocrinol. **17:**1681–1692.
55. **Xu, J., L. Liao, G. Ning, H. Yoshida-Komiya, C. Deng, and B. W. O'Malley.** 2000. The steroid receptor coactivator SRC-3 (p/CIP/RAC3/AIB1/ACTR/TRAM-1) is required for normal growth, puberty, female reproductive function, and mammary gland development. Proc. Natl. Acad. Sci. USA **97:**6379–6384.
56. **Yan, J., C. T. Yu, M. Ozen, M. Ittmann, S. Y. Tsai, and M. J. Tsai.** 2006. Steroid receptor coactivator-3 and activator protein-1 coordinately regulate the transcription of components of the insulin-like growth factor/AKT signaling pathway. Cancer Res. **66:**11039–11046.
57. **Yi, P., R. C. Wu, J. Sandquist, J. Wong, S. Y. Tsai, M. J. Tsai, A. R. Means, and B. W. O'Malley.** 2005. Peptidyl-prolyl isomerase 1 (Pin1) serves as a coactivator of steroid receptor by regulating the activity of phosphorylated steroid receptor coactivator 3 (SRC-3/AIB1). Mol. Cell. Biol. **25:**9687–9699.
58. **Yu, C., B. York, S. Wang, Q. Feng, J. Xu, and B. W. O'Malley.** 2007. An essential function of the SRC-3 coactivator in suppression of cytokine mRNA translation and inflammatory response. Mol. Cell **25:**765–778.
59. **Yuan, Y., L. Qin, D. Liu, R. C. Wu, P. Mussi, S. Zhou, Z. Songyang, and J. Xu.** 2007. Genetic screening reveals an essential role of p27kip1 in restriction of breast cancer progression. Cancer Res. **67:**8032–8042.
60. **Zhang, H., S. Q. Kuang, L. Liao, S. Zhou, and J. Xu.** 2004. Haploid inactivation of the amplified-in-breast cancer 3 coactivator reduces the inhibitory effect of peroxisome proliferator-activated receptor gamma and retinoid X receptor on cell proliferation and accelerates polyoma middle-T antigen-induced mammary tumorigenesis in mice. Cancer Res. **64:**7169–7177.
61. **Zhou, G., Y. Hashimoto, I. Kwak, S. Y. Tsai, and M. J. Tsai.** 2003. Role of the steroid receptor coactivator SRC-3 in cell growth. Mol. Cell. Biol. **23:**7742–7755.
62. **Zhou, H. J., J. Yan, W. Luo, G. Ayala, S. H. Lin, H. Erdem, M. Ittmann, S. Y. Tsai, and M. J. Tsai.** 2005. SRC-3 is required for prostate cancer cell proliferation and survival. Cancer Res. **65:**7976–7983.